

4

**DEPARTMENT OF DEFENSE  
Electromagnetic Compatibility Analysis Center  
Annapolis, Maryland 21402**

AN ANALYSIS OF PROPAGATION IN A SURFACE DUCT  
OVER A PERIODICALLY ROUGH EARTH

AD-A220 565



FEBRUARY 1990

TECHNICAL REPORT

Prepared by

Sherman W. Marcus and Michael L. Haberman

**IIT Research Institute  
Under Contract to  
Department of Defense**

**SDTIC  
ELECTE  
APR 19 1990  
B D**

Approved for public release; distribution is unlimited.

**UNCLASSIFIED**

SECURITY CLASSIFICATION OF THIS PAGE

REPORT DOCUMENTATION PAGE				
1a. REPORT SECURITY CLASSIFICATION <b>UNCLASSIFIED</b>		1b. RESTRICTIVE MARKINGS		
2a. SECURITY CLASSIFICATION AUTHORITY		3. DISTRIBUTION/AVAILABILITY OF REPORT  Approved for public release; distribution is unlimited.		
2b. DECLASSIFICATION/DOWNGRADING SCHEDULE				
4. PERFORMING ORGANIZATION REPORT NUMBER(S) ECAC-TR-88-001		5. MONITORING ORGANIZATION REPORT NUMBER(S)		
6a. NAME OF PERFORMING ORGANIZATION DoD Electromagnetic Com- patibility Analysis Center	6b. OFFICE SYMBOL (If applicable)	7a. NAME OF MONITORING ORGANIZATION		
6c. ADDRESS (City, State and Zip Code) North Severn Annapolis, MD 21402-1187		7b. ADDRESS (City, State and Zip Code)		
8a. NAME OF FUNDING/SPONSORING ORGANIZATION	8b. OFFICE SYMBOL (If applicable)	9. PROCUREMENT INSTRUMENT IDENTIFICATION NUMBER F-19628-85-C-0071 CDRL # 10P		
8c. ADDRESS (City, State and Zip Code)		10. SOURCE OF FUNDING NOS.		
		PROGRAM ELEMENT NO.	PROJECT NO. P0813	TASK NO. 5
				WORK UNIT NO.
11. TITLE (Include Security Classification) AN ANALYSIS OF PROPAGATION IN A SURFACE DUCT OVER A PERIODICALLY ROUGH EARTH				
12. PERSONAL AUTHOR(S) Sherman W. Marcus, Ph.D., and Michael L. Haberman, Ph.D.				
13a. TYPE OF REPORT TECHNICAL REPORT	13b. TIME COVERED From _____ To _____	14. DATE OF REPORT (Yr., Mo., Day) 1990 FEBRUARY	15. PAGE COUNT 84	
16. SUPPLEMENTARY NOTATION				
17. COSATI CODES		18. SUBJECT TERMS (Continue on reverse if necessary and identify by block number)		
FIELD	GROUP	PROPAGATION, ROUGH-EARTH DUCTING, ROUGH-BOUNDARY		
20	14	WAVEGUIDE; SURFACE DUCT.		
19. ABSTRACT (Continue on reverse if necessary and identify by block number)  A mathematical model for determining the effects of a small sinusoidal roughness on horizontally polarized radio waves, propagating over large distances in a horizontally homogenous tropospheric duct, is presented. The wave equation is solved for the appropriate boundary conditions. The eigenvalues of the solution are the roots of an infinite determinant. An effective reflection coefficient is derived and used with the infinite determinant to obtain an "equivalent zero mode matrix", from which the eigenvalues can be obtained. A perturbation method is then used (Cont.)				
20. DISTRIBUTION/AVAILABILITY OF ABSTRACT UNCLASSIFIED/UNLIMITED <input checked="" type="checkbox"/> SAME AS RPT. <input type="checkbox"/> DTIC USERS <input type="checkbox"/>		21. ABSTRACT SECURITY CLASSIFICATION <b>UNCLASSIFIED</b>		
22a. NAME OF RESPONSIBLE INDIVIDUAL T. Treadway		22b. TELEPHONE NUMBER (Include Area Code) 301-267-2354 A/V-281-2354	22c. OFFICE SYMBOL XM	

DD FORM 1473, 87 JAN

EDITION OF 83 APR 15 OBSOLETE

**UNCLASSIFIED**

19. ABSTRACT (Continued)

to derive a computationally efficient means of calculating the eigenvalues from the equivalent matrix. Examples that demonstrate that the attenuation due to the roughness can be significant are provided.

EXECUTIVE SUMMARY

The prediction of electromagnetic field strengths at large distances from a radiating antenna is important to designers and users of communications systems. Such field strengths can be greatly influenced by the variation of the modified atmospheric refractivity  $M$  with height  $z$ . If the gradient of  $M$  is negative over a range of  $z$ , an extreme enhancement in field strength may be realized at large distances from the source. The layer of the atmosphere responsible for the enhancement is known as a duct. When the ground is the lower boundary of the ducting layer, the duct is called a surface, or ground-based, duct; otherwise, it is denoted as an elevated duct. One common type of surface duct is found over the ocean and is known as an evaporation duct. Since the propagation of electromagnetic waves is sensitive to the phase of plane wave spectral components, which can be greatly influenced by the form of the reflecting ground, ground roughness is expected to have an important effect on the field strengths.

As a first step toward developing a mathematical model for duct propagation over a general rough earth, the problem considered herein is of a perfectly conducting periodic ground with a small roughness amplitude on the lower boundary of a duct. Specifically, the wave equation is developed and solved for the two-dimensional case of a long horizontal source. This method is applied to the problem of a long horizontal source radiating over a sinusoidally shaped, perfectly conducting ground within a surface duct environment. The eigenvalues of the "rough-walled waveguide" are found by expanding a characteristic determinant about zero roughness amplitude to obtain an "equivalent zero mode matrix". It is shown that for the specular component of the reflection, the problem can be considered in terms of an effective reflection coefficient that accounts for re-scattering of energy back into the specular direction.

<b>Accession For</b>	
NTIS GRA&I	<input checked="" type="checkbox"/>
DTIC TAB	<input type="checkbox"/>
Unannounced	<input type="checkbox"/>
Justification	
By _____	
Distribution/ _____	
<b>Availability Codes</b>	
Dist	Avail and/or Special
A-1	

An eigenvalue perturbation method is developed using the equivalent matrix that permits the calculation of eigenvalues for the rough-earth case using those of the smooth-earth case. It is shown that the eigenvalue perturbation scheme is as accurate as directly obtaining the eigenvalues from the equivalent matrix but requires much less computation time. The relationship between the two methods has been detailed, and the eigenvalue perturbations, as well as roughness loss rates, have been shown to be consistent with results obtained using a rough-earth form of the fundamental waveguide mode equation.

The methods documented in this report are a first step toward developing a mathematical model of propagation under the given conditions. They can be considered a research model applicable to a limited set of circumstances. Further work is needed to extend the model and make it more widely applicable.

PREFACE

The Electromagnetic Compatibility Analysis Center (ECAC), a Department of Defense facility, was established to provide advice and assistance on electromagnetic compatibility matters to the Secretary of Defense, the Joint Chiefs of Staff, the military departments, and other DoD components. The Center, located at North Severn, Annapolis, Maryland 21402, is under the policy control of the Assistant Secretary of Defense for Communication, Command, Control, and Intelligence, and the Chairman, Joint Chiefs of Staff, or their designees, who jointly provide policy guidance, assign projects, and establish priorities. ECAC functions under the executive direction of the Secretary of the Air Force, and the management and technical direction of the Center are provided by military and civil service personnel. The technical support function is provided through an Air Force-sponsored contract with the IIT Research Institute (IITRI).

To the extent possible, all abbreviations and symbols used in this report are taken from the American National Standards Institute, Inc., American National Standard ANSI (Y10.19) 1969 Letter Symbols for Units Used in Science and Technology.

Users of this report are invited to submit comments that would be useful in revising or adding to this material to the Director, ECAC, North Severn, Annapolis, Maryland 21402-1187, Attention: XM.

TABLE OF CONTENTS

<u>Subsection</u>	<u>Page</u>
GLOSSARY.....	xi
SECTION 1	
INTRODUCTION	
BACKGROUND.....	1-1
OBJECTIVE.....	1-3
APPROACH.....	1-3
ORGANIZATION OF THE DOCUMENT.....	1-5
SECTION 2	
GENERAL FORMULATION	
GENERAL.....	2-1
PROPAGATION MEDIA AND ROUGH BOUNDARY.....	2-1
FIELD EQUATIONS.....	2-3
PLANE WAVE SPECTRUM REPRESENTATION.....	2-5
SOLUTIONS OF THE EQUATIONS.....	2-9
SUMMARY.....	2-18
SECTION 3	
EFFECTIVE REFLECTION COEFFICIENT AND WAVEGUIDE MODE ATTENUATION	
GENERAL.....	3-1
REFLECTION COEFFICIENTS.....	3-1
WAVEGUIDE MODE EQUATION.....	3-5
EIGENVALUE PERTURBATIONS.....	3-9
TRAPPED MODES.....	3-11
PROPAGATION LOSS RATE.....	3-13
SUMMARY.....	3-15

TABLE OF CONTENTS (Continued)

<u>Subsection</u>	<u>Page</u>
SECTION 4	
SOLUTION FOR SINUSOIDAL ROUGHNESS	
GENERAL.....	4-1
EQUIVALENT ZERO MODE MATRIX.....	4-4
EIGENVALUE PERTURBATIONS AND PROPAGATION LOSS RATES.....	4-8
SECTION 5	
DISCUSSION AND RESULTS	
	5-1
SECTION 6	
SUMMARY	
	6-1

LIST OF ILLUSTRATIONS

<u>Figure</u>		
2-1	Physical model for duct calculations over periodic rough earth.....	2-2
2-2	Contour for integral of Equation 2-47.....	2-17
2-3	Schematic location of smooth surface eigenvalues for different Floquet contributions.....	2-20
3-1	Physical model for duct calculations over sinusoidal rough earth.....	3-2
3-2	Discrete spectrum of plane wave reflection from sinusoidal rough surface.....	3-4
3-3	Mode scattering out of and into the <sup>(0)</sup> specular direction...	3-7
3-4	Roughness loss rate $L_{Sm}$ as a function of $d/\lambda$ for trapped modes of Figure 3-1, $\lambda = 4.4$ cm.....	3-16

TABLE OF CONTENTS (Continued)

Figure Page

LIST OF ILLUSTRATIONS (Continued)

5-1	Roughness loss rate $L_{Sm}$ as a function of $d/\lambda$ for trapped propagation modes within duct of Figure 5-2, using each of the computational models.....	5-2
5-2	Physical model for duct calculations over sinusoidal rough earth.....	5-3
5-3	The effective reflection coefficient of sinusoidal ground for amplitude $\epsilon = 0.1$ m, frequency = 6.814 GHz for different values of $d/\lambda$ .....	5-4
5-4	Field relative to free space within duct of Figure 5-2 $f = 6.814$ GHz, $ x  = 66.7$ km, over smooth earth and over sinusoidal rough earth, $\epsilon = 0.1$ m.....	5-6

LIST OF REFERENCES R-1

## GLOSSARY

- duct - a nonstandard condition in the troposphere whereby a layer is formed, the refractivity gradient of which is less than  $-157$  N units/km, causing the ray curvature of a radio wave to be greater than the earth's curvature, with the result that the wave is trapped in the layer and propagated beyond its normal range
- elevated duct - a duct, the bottom of which is above the earth's surface
- evaporation duct - a surface duct formed above a body of water when evaporation causes a moist air layer to form under a dry layer
- Floquet series - a discrete sum of plane waves used as part of the solution of a differential equation with periodic boundary conditions
- index of refraction,  $n$  - ratio of the phase velocity of an electromagnetic wave in free space to the phase velocity in a medium
- modified refractivity,  $M$  - defined by the equation  $M = N + (h/r) \cdot 10^6$ , where  $N$  is the refractivity,  $h$  is the height, and  $r$  is the earth's radius.  $M$  is defined in terms of  $N$  so that its gradient is negative in a duct.
- perturbation expansion - expansion of the rough-earth eigenvalues in terms of the smooth-earth ones as a series in the roughness height parameter, valid for small values of the roughness height

GLOSSARY (Continued)

- refractivity, N - defined for convenience by the equation  $(n-1) \cdot 10^6$ , where n is the index of refraction
- refractivity profile - a plot of refractivity (either N or M) versus height, where refractivity is the abscissa and height is the ordinate
- specular reflection - reflection that is the same type as that caused by smooth surfaces and has the following properties: it is directional (angle of incidence equals the angle of reflection), its phase is coherent, and its fluctuations have a relatively small amplitude
- surface duct - a duct with a bottom that is on the earth's surface and a modified refractivity gradient that is negative from the earth's surface to the duct top

SECTION 1  
INTRODUCTION

BACKGROUND

The prediction of electromagnetic field strengths at large distances from a radiating antenna is important to designers and users of communications systems. Such field strengths can be greatly influenced by the variation of the modified atmospheric refractivity  $M$  with height  $z$ . If  $dM/dz$  is negative over a range of  $z$ , the field strength can be enhanced at large distances from the source. The layer of the atmosphere responsible for the enhancement is called a duct.<sup>1-1</sup> When the ground is the lower boundary of the ducting layer, the duct is called a surface, or ground-based, duct. Otherwise, it is denoted as an elevated duct. One common type of surface duct is found over the ocean and is known as an evaporation duct.<sup>1-2</sup>

Numerical methods for predicting field strengths at large distances from a radiating source in surface and elevated ducts have been documented.<sup>1-3,1-4</sup> These methods are based on the waveguide mode theory of wave propagation<sup>1-5</sup> and assume horizontal homogeneity of the tropospheric layers and a smooth earth. Since the ducted modes are sensitive functions of the phase of plane

---

<sup>1-1</sup>Kerr, D. E., "Propagation of Short Radio Waves," MIT Radiation Laboratory Series, Vol. 13, McGraw Hill, New York, 1951.

<sup>1-2</sup>Rotheram, S., "Radiowave Propagation in the Evaporation Duct," The Marconi Review, Vol. 37, No. 192, 1974, pp. 18-40.

<sup>1-3</sup>Marcus, S. W., "A Model to Calculate EM Fields in Tropospheric Duct Environments at Frequencies through SHF," Radio Science, Vol. 17, No. 5, 1982, pp. 885-901.

<sup>1-4</sup>Marcus, S. W., and Stuart, W. D., A Model to Calculate EM Fields in Tropospheric Duct Environments at Frequencies through SHF, ESD Technical Report 81-102, AD-A107710, DoD ECAC, Annapolis, MD, September 1981.

<sup>1-5</sup>Budden, K. G., The Wave Guide Mode Theory of Wave Propagation, Logos Press, Ltd., London, 1961.

wave spectral components, which can be greatly influenced by the form of the reflecting ground, ground roughness is expected to have an important effect on these modes.

A method for considering ground roughness in waveguide models of duct propagation has been developed and utilized by Rotheram (Reference 1-2) and Hitney.<sup>1-6</sup> In the expression for the boundary conditions at the ground, this method replaces the Fresnel reflection coefficient by the effective reflection coefficient of a randomly rough surface as developed by Rice<sup>1-7</sup> and Ament<sup>1-8</sup> and verified by Beard.<sup>1-9</sup>

For the case of a horizontally polarized wave incident on a perfect conductor, the Fresnel reflection coefficient is -1, while the effective reflection coefficient is

$$\bar{R} = -1 + 1/2 (\Delta\phi)^2 \quad (1-1)$$

where the Rayleigh factor  $\Delta\phi$  is defined as

$$\Delta\phi = 2 k h \sin \theta \quad (1-2)$$

$k$  is the free-space wave number,  $h$  is the root-mean-square (rms) bump height of the roughness, and  $\theta$  is the grazing angle of the ray representing the incident plane wave.

---

<sup>1-6</sup>Hitney, H., et al., "Tropospheric Radio Propagation Assessment," Proceedings of the IEEE, Vol. 73, No. 2, 1985, pp. 265-283.

<sup>1-7</sup>Rice, S. O., "Reflection of Electromagnetic Waves from Slightly Rough Surfaces," The Theory of Electromagnetic Waves, M. Kline, ed., Interscience Publishers, New York, NY, 1951, p. 351.

<sup>1-8</sup>Ament, W. D., "Toward a Theory of Reflection by a Rough Surface," Proceedings of the IRE, Vol. 41, No. 1, 1953, pp. 142-146.

<sup>1-9</sup>Beard, C. I., "Coherent and Incoherent Scattering of Microwaves from the Ocean," IRE Transactions on Antennas and Propagation, Vol. AP-9, No. 5, 1961, pp. 470-483.

This effective coefficient considers only reflection in the specular direction. It is an expression of the amount of energy scattered out of that direction by the ground roughness and it contains the assumption of a standard atmosphere with no ducts. This method of considering ground roughness when ducts are present is popular in spite of its "semi-quantitativeness" (Reference 1-6). One difficulty in justifying its use is based on the dependency of waveguide modes upon continuous reflection from the waveguide walls (Reference 1-5). Thus, a portion of the energy scattered out of the specular direction at one reflection from the ground may be scattered back into the original specular direction at a later reflection from the ground. In addition, because of the nature of the duct, energy scattered out of the specular direction may continue to propagate and may represent a mode in its own right. Finally, the effective reflection coefficient was derived and experimentally verified for real angles of incidence. Its carryover to the complex eigenangles characteristic of the waveguide formulation of duct propagation has not been validated.

#### OBJECTIVE

The objective of this analysis was to develop a first-degree approximation for estimating the electromagnetic field strengths at large distances from a radiating antenna that is within a surface duct situated over a periodically rough ground.

#### APPROACH

As a first step toward developing a mathematical model for duct propagation over a general rough earth, the problem considered herein is of a perfectly conducting periodic ground with a small roughness amplitude below a duct environment. The wave equation is developed and solved for the two-dimensional case of a long, horizontal line source. The eigenvalues of the solution are the roots of an infinite determinant that reduce to the smooth-earth eigenvalues as the ground roughness approaches zero. Because it is

infinite-dimensional, the determinant cannot be evaluated directly and the eigenvalue must be calculated using other means.

Towards this, an expression for the ground reflection coefficient analogous to Equation 1-1 is derived that accounts for the dispersive nature of the ground-reflected field, as well as the multiple reflections characteristic of waveguide modes. This effective reflection coefficient is obtained for the case of horizontally polarized radio waves propagating over a sinusoidally shaped, perfectly conducting ground within a surface duct environment.

This reflection coefficient is then used in conjunction with the fundamental waveguide mode equation to derive an eigenvalue perturbation method wherein the eigenvalues for propagation over rough earth can be obtained easily from the smooth-earth eigenvalues. A simple numerical expression is obtained for this eigenvalue perturbation in terms of ground and atmospheric reflection coefficients. Although the fundamental waveguide mode equation approach is entirely equivalent to the formulation based on the wave equation,<sup>1-10</sup> the waveguide mode formulation provides greater physical insight into the waveguide phenomena. This waveguide mode formulation also leads to a closed-form expression for the rate of modal attenuation due to roughness for trapped modes in a surface duct formed by a bilinear refractivity profile.

Another expression for the eigenvalues is then derived by expanding a characteristic determinant about zero roughness amplitude to obtain an "equivalent matrix" for propagation over rough earth which is identical in form to the characteristic matrix for smooth-earth propagation. It is shown that for the specular component of the reflection, the problem can be considered in terms of an effective reflection coefficient that accounts for rescattering of energy back into the specular direction. (The determination

---

<sup>1-10</sup>Marcus, S. W., "Propagation in a Surface Duct Over a Two-Dimensional Sinusoidal Earth," Radio Science, Vol. 23, No. 6, 1988, pp. 1039-1047.

of field contributions due to the portion of energy scattered out of the specular direction and not rescattered back into that direction will be relegated to a future study.)

A perturbation technique is used to derive an expression for the eigenvalues of the rough-earth case in terms of the smooth-earth eigenvalues from the equivalent matrix. This eliminates the necessity of a separate, time-consuming search for the roots of the characteristic determinant of the equivalent matrix for each set of roughness parameters. The accuracy of this perturbation method is discussed, particularly as it relates to the attenuation of trapped modes in surface ducts due to the roughness.

Numerical field strength predictions are presented with and without the sinusoidal ground roughness, which shows that attenuation due to roughness can be significant. A comparison is also made between predictions for which the complete reflection coefficient is used and those for which only scattering out of the specular direction is considered.

#### ORGANIZATION OF THE DOCUMENT

In Section 2, the field equation for a horizontally polarized wave propagating in a duct situated over a perfectly conducting, periodically rough ground with small amplitude is derived. The solution to this equation is given in the form of a Floquet series. The formal solution is dependent on determining eigenvalues that are the roots of an infinite determinant. It remains to develop practical means of determining the roots. Theoretical concepts required to achieve this are derived in Section 3 and the actual solution is obtained in Section 4.

In Section 3, a waveguide mode formulation is used to derive an effective ground reflection coefficient when the roughness is sinusoidal. This coefficient is used in the fundamental waveguide mode equation to determine eigenvalues of the rough waveguide as a perturbation of the smooth-earth values. The roughness is found to cause attenuation of trapped modes, and

this attenuation is expressed in a simple manner. This expression reduces to a closed form when the duct is approximated by a bilinear refractivity profile.

For the same sinusoidal roughness, the specular contribution to the field equations of Section 2 are derived in Section 4. This is done by deriving an "equivalent zero mode matrix" from the infinite determinant using the effective reflection coefficient. This accounts for scattering both out of and into the specular direction. A computationally efficient means of obtaining the relevant eigenvalues from the equivalent matrix as perturbations of the smooth-earth ones are derived. It should be noted that this perturbation expansion is not the one mentioned in the previous paragraph. Once again, expressions for loss rates are obtained.

In Section 5, numerical results obtained directly from the equivalent matrix and from the eigenvalue perturbation methods are compared. This is done by first plotting roughness loss rates of individual trapped modes, obtained from the two methods, and then plotting field strengths using the four lowest order modes.

Section 6 contains a summary of the report.

## SECTION 2 GENERAL FORMULATION

### GENERAL

References 1-3 and 1-4 contain the mathematical formulation for describing an electromagnetic wave propagation in a tropospheric duct over a smooth earth. This formulation will now be extended to include a periodically rough boundary condition between the earth and the troposphere. Solutions to the field equations will be obtained using a Floquet series. These solutions will be dependent on determining the eigenvalues that are the roots of an infinite determinant. Determination of the eigenvalues will be discussed in Section 4.

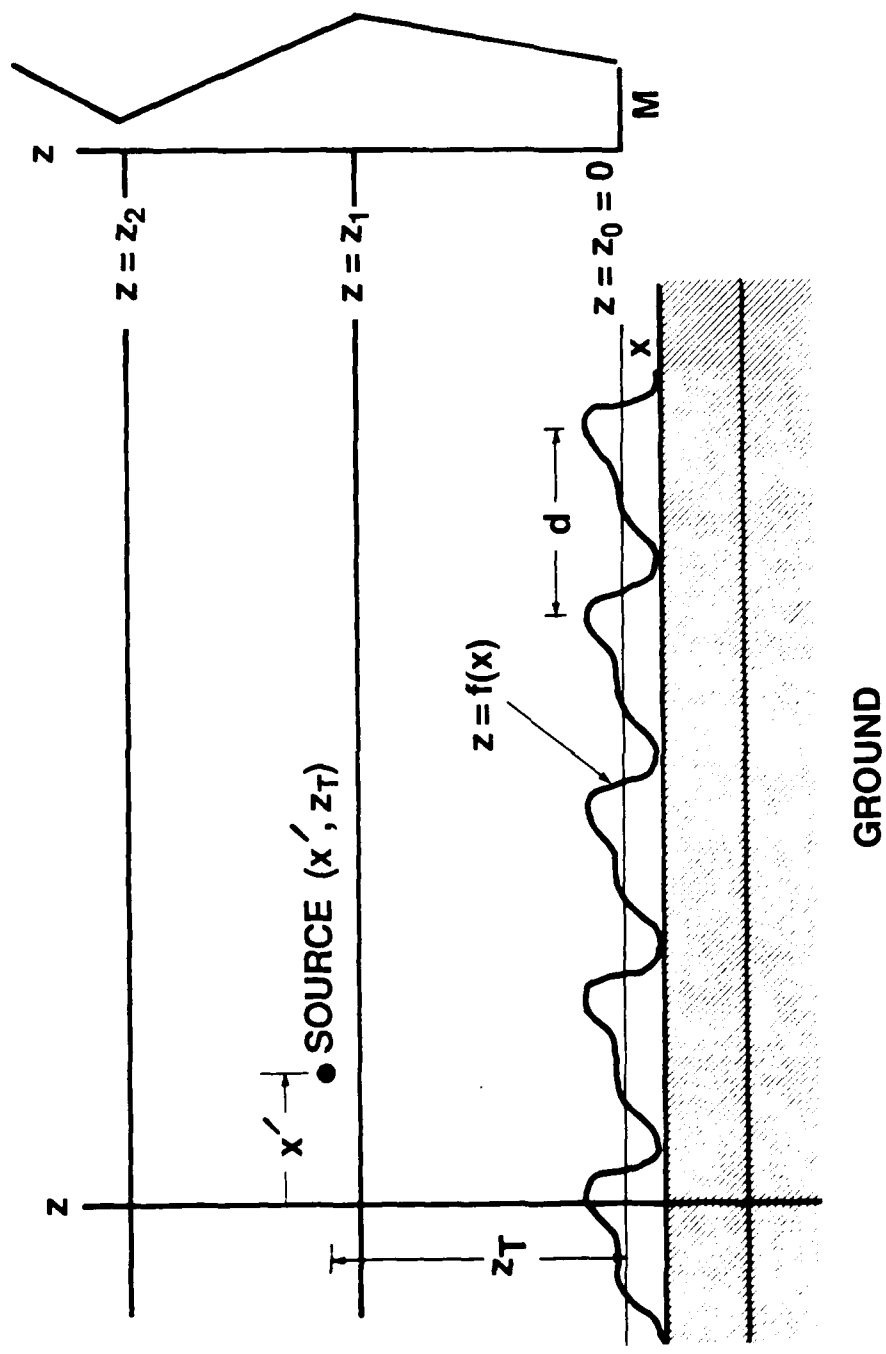
### PROPAGATION MEDIA AND ROUGH BOUNDARY

The modified index of refraction  $m(z)$  is defined as

$$m(z) = M(z) \times 10^{-6} + 1 = n(z) + z/a \quad (2-1)$$

where  $n(z)$  is the actual index of refraction;  $a$  is the radius of the earth in the same units as the height  $z$ ; and the  $z/a$  term compensates for earth curvature, thereby enabling the use of Cartesian coordinates (Reference 1-1).

The modified refractivity profile (i.e., its variation with height) will be approximated by a continuous piecewise linear profile with  $L$  sections (see Figure 2-1). Each section will represent an atmospheric layer, or region, the boundaries of which are parallel to a flat earth located at  $z = z_0 = 0$ . The interface between the  $i$ -th and  $i$ -th + 1 layer is located at  $z = z_i$  ( $1 \leq i \leq L - 1$ ), with the layer  $i = 1$  closest to the ground. The  $L$ -th layer is unbounded in the positive  $z$  direction.



**GROUND**

Figure 2-1. Physical model for duct calculations over periodic rough earth.

In each atmospheric layer,

$$m_i^2(z) \approx 1 + (z - H_i) \tan \alpha_i, \quad 1 \leq i \leq L \quad (2-2)$$

where  $H_i$  is the value of  $z$  at which  $m_i(z)$  would equal unity and the slope  $(\tan \alpha_i)/2$  of the  $m_i$  versus  $z$  curve is assumed small.

It is assumed that the boundary between the atmosphere and the infinitely conductive ground is rough in a periodic manner with spatial period  $d$ . This boundary can be described in terms of a Fourier series.

#### FIELD EQUATIONS

The source of a horizontally polarized wave can be considered to be a linear density of magnetic dipoles  $\vec{p}$  of infinite length that is uniformly distributed along a line parallel to the  $y$  axis, oriented in the  $z$  direction, and located at  $x = x'$ ,  $z = z_T$  (see Figure 2-1). In a laterally homogeneous medium, the fields due to such a source may be obtained from the  $z$ -directed magnetic Hertz potential vector:

$$\vec{\Pi} = \Pi(x,z) \hat{z} \quad (2-3)$$

and

$$\vec{E} = -j\omega\mu_0 \nabla \times \vec{\Pi}, \quad \vec{H} = \nabla \times \nabla \times \vec{\Pi} \quad (2-4)$$

where  $\omega = 2\pi f$ ,  $f$  is the frequency of the wave,  $\mu_0$  is the permeability in vacuum, and a sinusoidal time dependence is assumed. In the  $i$ -th layer of the atmosphere,  $\Pi(x,z)$  will satisfy the inhomogeneous Helmholtz equation:

$$\nabla^2 \pi_i + k_{m_i}^2(z) \pi_i = J(x,z)/(j\omega\mu_0), \quad 1 \leq i \leq L \quad (2-5)$$

where the source term is given by

$$J(x,z) = -j\omega\mu_0 p \delta(x-x') \delta(z-z_T) \quad (2-6)$$

$k = \omega(\mu_0\epsilon_0)^{1/2}$  is the wave number in free space, and  $\epsilon_0$  is the permittivity in vacuum.

The  $\pi_i$  satisfy the following boundary conditions which, using Equation 2-4, expresses the continuity across the region boundaries of the components of  $\vec{E}$  and  $\vec{H}$  parallel to the boundaries:

$$\pi_i = \pi_{i+1} \quad \text{for } z = z_i, \quad 1 \leq i \leq L-1 \quad (2-7)$$

$$\partial\pi_i/\partial z = \partial\pi_{i+1}/\partial z$$

Since it is assumed that the ground conductivity is infinite, the boundary condition at the ground is

$$\hat{n} \times \vec{E} = 0 \quad \text{for } z = f(x) \quad (2-8)$$

where  $\hat{n}$  is the unit outward normal to the surface and  $f(x)$  is a periodic function that describes the earth's rough boundary. Using Equation 2-4, this can be expressed as

$$\Pi_1(x,z) = 0 \quad \text{for } z = f(x) \quad (2-9)$$

When  $z$  is small,  $\Pi_1(x,z)$  may be expanded in a Taylor series about  $z = 0$  to yield

$$\Pi_1(x,0) + [\partial \Pi_1(x,0) / \partial z] f(x) + [\partial^2 \Pi_1(x,0) / \partial z^2] f(x)^2 / 2 + \dots = 0 \quad (2-10)$$

which, together with Equation 2-7, are the boundary conditions for the problem.

#### PLANE WAVE SPECTRUM REPRESENTATION

For the smooth earth problem, a Fourier transform formalism may be used to eliminate the horizontal  $x$  variable, thereby transforming the partial differential equation into an ordinary differential equation (Reference 1-4). This formalism requires horizontal homogeneity for its implementation, which is not present in the problem under consideration because of the presence of ground roughness. (This is not to be confused with the atmospheric layers, which are horizontally homogeneous and which thereby permit the use of the Hertz potential formalism.) Therefore, an analogous method will be used that is valid for the periodic type of boundary that is assumed. This method will reduce to the Fourier transform formalism in the zero roughness limit.

The source function  $J(x,z)$  may be written as a sum of its plane wave spectral components. Since these components are continuously distributed, this sum is expressed as an integral:

$$J(x,z) = \frac{1}{(2\pi)} \int_{-\infty}^{\infty} d\mu e^{j\mu x} \tilde{J}(\mu,z) \quad (2-11)$$

where, using the definition of the Fourier transform and Equation 2-6,

$$\begin{aligned} \tilde{J}(\mu,z) &= \frac{1}{(2\pi)} \int_{-\infty}^{\infty} dx e^{-j\mu x} J(x,z) \\ &= -j \omega \mu_0 p \delta(z - z_T) e^{-j\mu x'} \end{aligned} \quad (2-12)$$

Each spectral component  $\tilde{J}(\mu,z)e^{j\mu x}/(2\pi)$  may be considered an independent source contributing to the electric field. Let the solution of the problem for this component of the source be given by  $\tilde{\pi}_i(\mu,x,z)e^{j\mu(x-x')}/(2\pi)$  in the  $i$ -th atmosphere layer; then, by superposition, the solution of the problem for all the source components is

$$\pi_i(x,z) = \frac{1}{(2\pi)} \int_{-\infty}^{\infty} d\mu e^{j\mu(x-x')} \tilde{\pi}_i(\mu,x,z) \quad (2-13)$$

This equation differs from the familiar Fourier transform in that  $\tilde{\pi}_i$  is a function of  $x$  as well as  $\mu$  and  $z$ .

Since the solution of the problem in the  $i$ -th layer is  $\tilde{\pi}_i(\mu,x,z)e^{j\mu(x-x')}$  when the source function is  $\tilde{J}(\mu,z)e^{j\mu x}$ , these may be substituted into Equation 2-5 for the  $\pi_i$  and  $J$ , respectively. Carrying out the differentiation of the  $e^{j\mu x}$  factor and using Equation 2-12 then results in

$$\begin{aligned} &(\partial^2/\partial x^2 + \partial^2/\partial z^2)\tilde{\pi}_i + 2j\mu \partial\tilde{\pi}_i/\partial x + (k_{m_i}^2 - \mu^2)\tilde{\pi}_i \\ &= -p \delta(z - z_T) \end{aligned} \quad (2-14)$$

The  $e^{j\mu(x-x')}$  factor no longer appears in Equation 2-14. The only source of variation in the  $x$  direction is due to the periodic rough earth boundary condition. Hence, the variation of  $\tilde{\Pi}$  with  $x$  is periodic and may be written in the form:

$$\tilde{\Pi}_i(\mu, x, z) = \sum_n F_i^{(n)}(\mu, z) e^{j\kappa n x} \quad (2-15)$$

Substituting this form of the solution into Equation 2-14 results in

$$\begin{aligned} \sum_n \{ d^2 F_i^{(n)} / dz^2 + [k^2 m_i^2 - (\mu + \kappa n)^2] F_i^{(n)} \} e^{j\kappa n x} \\ = -\rho \delta(z - z_T) \end{aligned} \quad (2-16)$$

This equation could have been obtained directly from Equation 2-5 by assuming a solution of the form:

$$\Pi_i = \sum_n F_i^{(n)}(\mu, z) e^{j(\mu + \kappa n)x} \quad (2-17)$$

This equation is a Floquet series. It is a discrete sum of plane waves because the boundary conditions are periodic.

Since the  $m_i$  are not functions of  $x$ , the coefficients of  $\exp(j\kappa n x)$  in Equation 2-16 are independent. Therefore, the sum of  $N$  terms are  $N$  independent differential equations. The result is

$$d^2 F_i^{(n)} / dz^2 + [k^2 m_i^2(z) - \mu^{(n)2}] F_i^{(n)} = -\delta_{no} \rho \delta(z - z_T), \text{ all } n \quad (2-18)$$

where

$$\mu^{(n)} \equiv \mu + \kappa n \quad (2-19)$$

From Equation 2-17, it is seen that the expression for  $\Pi_i$  is the same in each atmospheric region except for the  $F_i^{(n)}$  factor. Hence, the boundary conditions in Equation 2-7 can be rewritten in the same form but with  $\Pi_i$  replaced by  $F_i^{(n)}$ :

$$F_i^{(n)} = F_{i+1}^{(n)} \quad \text{for } z = z_i, 1 \leq i \leq L-1 \quad (2-20)$$

$$\partial F_i^{(n)} / \partial z = \partial F_{i+1}^{(n)} / \partial z$$

The expression of the boundary condition of Equation 2-10 is somewhat more involved because of its dependence on  $x$ . Using Equation 2-17, this boundary condition becomes

$$\sum_n e^{j\kappa n x} \left\{ F_1^{(n)}(\mu, 0) + \partial F_1^{(n)}(\mu, 0) / \partial z f(x) + \partial^2 F_1^{(n)}(\mu, 0) / \partial z^2 f(x)^2 / 2 + \dots \right\} = 0 \quad (2-21)$$

or, ignoring terms of order  $f(x)^3$  and higher,

$$\sum_n \left\{ e^{j\kappa n x} F_1^{(n)}(\mu, 0) + \partial F_1^{(n)}(\mu, 0) / \partial z \sum_m p_m e^{j\kappa(m+n)x} - \frac{1}{2} \gamma^{(n)} \partial^2 F_1^{(n)}(\mu, 0) \sum_m s_m e^{j\kappa(m+n)x} \right\} = 0 \quad (2-22)$$

where

$$\gamma^{(n)2} = k_{m_0}^2 - u^{(n)2} \quad (2-23)$$

and Equation 2-16 was used.  $p_m$  and  $s_m$  are the coefficients of the Fourier series of  $f(x)$  and  $f^2(x)$ , respectively, which are small for small roughness. Equation 2-22 will be simplified by using the orthonormality of functions of the form  $\exp(j2\pi nx/d)$ , expressed as:

$$\frac{1}{d} \int_0^d e^{j2\pi(m-n)x/d} dx = \delta_{mn} \quad (2-24)$$

Multiplying Equation 2-22 by  $e^{-jkrx}$  (where  $r$  is an integer) and integrating the result over the period  $d$  yields

$$\begin{aligned} F_1^{(r)}(\mu, 0) + \sum_n \partial F_1^{(n)}(\mu, 0) / \partial z p_{r-n} \\ - \frac{1}{2} \sum_n \gamma^{(n)2} F_1^{(n)}(\mu, 0) s_{r-n} = 0, \text{ all } r \end{aligned} \quad (2-25)$$

Therefore, to obtain a solution to the rough earth problem, Equation 2-18 must be solved using the boundary conditions in Equations 2-20 and 2-25.

### SOLUTIONS OF THE EQUATIONS

By substituting Equation 2-2, Equation 2-18 can be cast into the form of Stokes' equation, the solution of which is

$$F_i^{(n)}(\mu, z) = A_i^{(n)} K_1(q_i^{(n)}) + B_i^{(n)} K_2(q_i^{(n)}) + \tilde{F}_P \delta_{iP} \delta_{n0},$$

all  $n$  (2-26)

where

$$q_i^{(n)} = q_i^{(n)}(z) = \left( \frac{k}{|\tan \alpha_i|} \right)^{2/3} \left[ m_i^2(z) - \frac{\mu^{(n)2}}{k^2} \right] \quad (2-27)$$

$K_1$  and  $K_2$  are linear combinations of modified Hankel functions of order one-third,<sup>2-1</sup> and  $P$  is the number of the layer containing the source current. The  $A_i(n)$  and  $B_i(n)$  are functions of the parameter  $\mu$  and are found by invoking the boundary conditions. It is to be noted that, although  $\mu$  enters the differential Equation 2-18 in the form  $\mu^{(n)2}$ ,  $A_i(n)$  and  $B_i(n)$  cannot be written simply as functions of  $\mu^{(n)}$  since they must be found by solving a linear system of equations that include the boundary condition of Equation 2-25, which contains all values of  $n$ .

The particular solution  $\tilde{F}_p$  of the inhomogeneous form of Equation 2-18 (i.e.,  $n = 0$ ) is given by either of the following (Reference 1-3):

$$\tilde{F}_p = \begin{cases} R_p K_1(q_{p<}) K_2(q_{p>}) \\ - R_p K_1(q_{p>}) K_2(q_{p<}) \end{cases} \quad (2-28)$$

where

$$R_p = P/Wq_p'(z) \quad (2-29)$$

$$q_{p<} = q_p^{(0)}(\min\{z, z_T\}), \quad q_{p>} = q_p^{(0)}(\max\{z, z_T\}) \quad (2-30)$$

---

<sup>2-1</sup>Harvard Computational Laboratory, Tables of Modified Hankel Functions of Order One-Third and of Their Derivatives, Harvard University Press, Cambridge, MA, 1945.

W is the constant Wronskian of  $K_1$  and  $K_2$  defined by

$$W = W\{K_1, K_2\} = K_1(q_p) K_2'(q_p) - K_2(q_p) K_1'(q_p) \quad (2-31)$$

The primes in Equations 2-29 and 2-31 indicate differentiation with respect to the argument. In particular,

$$q_i^{(n)'}(z) \equiv dq_i^{(n)}(z)/dz \left( \frac{k}{|\tan \alpha_i|} \right)^{2/3} \tan \alpha_i \quad (2-32)$$

where Equations 2-2 and 2-27 were used. It should be noted that the right side of Equation 2-32 is independent of  $z$ ,  $u$ , and the index  $n$ .

To solve for the field in the atmospheric layers, the coefficients  $A_i^{(n)}$ ,  $B_i^{(n)}$  of the general solution in Equation 2-26 must be known. These will now be determined by solving a set of simultaneous linear equations obtained by substituting Equation 2-26 into the boundary condition of Equations 2-20 and 2-25. This will be accomplished here under the assumption that the source is not in the atmospheric layer bordering the ground, i.e.,  $P > 1$ . This assumption removes the necessity of considering the inhomogeneous solution of Equation 2-26 in the roughness boundary condition of Equation 2-25. It has no limiting effect for any finite height of the source, since the lowest layer can always be formally divided into two separate layers at a point below the source height. Substituting Equation 2-26 into Equation 2-25 yields:

$$\sum_n [A_1^{(r-n)} U_n^{(r-n)} + B_1^{(r-n)} V_n^{(r-n)}] = 0, \text{ all } r \quad (2-33)$$

where

$$\left. \begin{aligned} U_n^{(r-n)} &= K_1' q_1'(q_{10}^{(r-n)}) p_n + K_1(q_{10}^{(r-n)}) (\delta_{n0} - \frac{1}{2} r^{(r-n)2} s_n) \\ V_n^{(r-n)} &= K_2' q_1'(q_{10}^{(r-n)}) p_n + K_2(q_{10}^{(r-n)}) (\delta_{n0} - \frac{1}{2} r^{(r-n)2} s_n) \end{aligned} \right\} (2-34)$$

$$q_{ij}^{(n)} \equiv q_i^{(n)}(z_j) \tag{2-35}$$

Finally, substituting Equation 2-26 into Equation 2-20 yields

$$a_{2i,2i-1}^{(n)A_i} + a_{2i,2i}^{(n)B_i} + a_{2i,2i+1}^{(n)A_{i+1}} + a_{2i,2i+2}^{(n)B_{i+1}} = \beta_{2i}^{(n)} \tag{2-36}$$

and

$$\begin{aligned} a_{2i+1,2i-1}^{(n)A_i} + a_{2i+1,2i}^{(n)B_i} + a_{2i+1,2i+1}^{(n)A_{i+1}} \\ + a_{2i+1,2i+2}^{(n)B_{i+2}} = \beta_{2i+1}^{(n)} \end{aligned} \tag{2-37}$$

$1 \leq i \leq L-1$

where

$$\begin{aligned} a_{2i,2i-1}^{(n)} &= K_1(q_{ii}^{(n)}) \\ a_{2i,2i}^{(n)} &= K_2(q_{ii}^{(n)}) \\ a_{2i,2i+1}^{(n)} &= -K_1(q_{i+1,i}^{(n)}) \\ a_{2i,2i+2}^{(n)} &= -K_2(q_{i+1,i}^{(n)}) \end{aligned} \tag{2-38}$$

$$\begin{aligned}
 a_{2i+1,2i-1}^{(n)} &= K_1'(q_{ii}^{(n)}) \\
 a_{2i+1,2i}^{(n)} &= K_2'(q_{ii}^{(n)}) \\
 a_{2i+1,2i+1}^{(n)} &= -K_1'(q_{i+1,i}^{(n)})q_{i+1}' / q_i' \\
 a_{2i+1,2i+2}^{(n)} &= -K_2'(q_{i+1,i}^{(n)})q_{i+1}' / q_i'
 \end{aligned}
 \tag{2-39}$$

$$\begin{aligned}
 \beta_{2i}^{(n)} &= \tilde{F}_P(z=z_i) \delta_{n0} (\delta_{i+1,P} - \delta_{iP}) \\
 \beta_{2i+1}^{(n)} &= d\tilde{F}_P(z=z_i)/dz \delta_{n0} (\delta_{i+1,P} - \delta_{iP}) / q_i'
 \end{aligned}
 \tag{2-40}$$

and when  $i = L - 1$ , the  $A_{i+1}^{(n)}$  term is absent in order to satisfy the radiation condition.

Equations 2-33, 2-36, and 2-37 may be written in matrix form as

$$\alpha \eta = \beta \tag{2-41}$$

where  $\alpha$  is a square matrix, and  $\eta$  and  $\beta$  are column vectors. To illustrate their form, consider the case in which  $L = 2$ ,  $P = 2$ , and  $n$  takes on the values  $-1$ ,  $0$ , and  $1$ . By grouping together Equations 2-33, 2-36, and 2-37 for each value of  $n$ ,  $\alpha$  may be written

$$\alpha = \begin{bmatrix}
 a_{11}^{(-1)} & a_{12}^{(-1)} & & U_{-1}^{(0)} & V_{-1}^{(0)} & U_{-2}^{(1)} & V_{-2}^{(1)} \\
 a_{21}^{(-1)} & a_{22}^{(-1)} & a_{23}^{(-1)} & & & & \\
 a_{31}^{(-1)} & a_{32}^{(-1)} & a_{33}^{(-1)} & & & & \\
 U_1^{(-1)} & V_1^{(-1)} & & a_{11}^{(0)} & a_{12}^{(0)} & U_{-1}^{(1)} & V_{-1}^{(1)} \\
 & & & a_{21}^{(0)} & a_{22}^{(0)} & a_{23}^{(0)} & \\
 & & & a_{31}^{(0)} & a_{32}^{(0)} & a_{33}^{(0)} & \\
 U_2^{(-1)} & V_2^{(-1)} & & U_1^{(0)} & V_1^{(0)} & a_{11}^{(1)} & a_{12}^{(1)} \\
 & & & & & a_{21}^{(1)} & a_{22}^{(1)} & a_{23}^{(1)} \\
 & & & & & a_{31}^{(1)} & a_{32}^{(1)} & a_{33}^{(1)}
 \end{bmatrix} \tag{2-42}$$

and

$$\eta = \begin{bmatrix}
 A_1^{(-1)} \\
 B_1^{(-1)} \\
 B_2^{(-1)} \\
 A_1^{(0)} \\
 B_1^{(0)} \\
 B_2^{(0)} \\
 A_1^{(1)} \\
 B_1^{(1)} \\
 B_2^{(1)}
 \end{bmatrix} \quad
 \beta = \begin{bmatrix}
 0 \\
 0 \\
 0 \\
 0 \\
 B_2 \\
 B_3 \\
 0 \\
 0 \\
 0
 \end{bmatrix} \tag{2-43}$$

where

$$\begin{aligned} \beta_2 &= \tilde{F}_2(z=z_1) \\ \beta_3 &= [d\tilde{F}_2(z=z_1)/dz]/q_1' \end{aligned} \quad (2-44)$$

and

$$a_{11}^{(n)} = U_0^{(n)}, \quad a_{12}^{(n)} = V_0^{(n)} \quad (2-45)$$

Equation 2-41 is solved for any desired elements of  $n$  by using standard methods for solving a system of linear equations. Thus, following the definitions introduced for the smooth-earth case (Reference 1-3), the coefficients  $A_i^{(n)}$ ,  $B_i^{(n)}$  may be written as ratios of determinants:

$$A_i^{(n)} = ||\tau_{Ai}^{(n)}|| / ||\alpha||, \quad B_i^{(n)} = ||\tau_{Bi}^{(n)}|| / ||\alpha|| \quad (2-46)$$

where  $\tau_{Ai}^{(n)}$  is the matrix obtained by replacing the column of  $\alpha$  containing the coefficient  $A_i^{(n)}$  by the vector  $\beta$ , and  $\tau_{Bi}^{(n)}$  is the matrix obtained by replacing the column of  $\alpha$  containing the  $B_i^{(n)}$  coefficient by the vector  $\beta$ . The  $||\tau||$  are functions of the source height  $z_T$ , while  $||\alpha||$  is not.

The above values of  $A_i^{(n)}$ ,  $B_i^{(n)}$  can be substituted into Equation 2-26 to obtain the  $F_i^{(n)}$ , which are used, in turn, to obtain  $\tilde{\Pi}$  from Equation 2-15. This result is then used in Equation 2-13 to obtain the desired Hertz potential. In the event that the ground were smooth, all the  $F_i^{(n)}$  would reduce to 0 for all  $n \neq 0$ . Since only  $n = 0$  would be included,  $F_i^{(0)}(\nu, z)$  would be obtained. Far from the source, the expression for the electric field relative to its free space value is proportional to  $\Pi$  and is precisely the

same as that for the cylindrically symmetric smooth-earth case (Reference 1-3).

From Equations 2-13, 2-15, and 2-26,

$$\pi_i(x, z) = \frac{1}{2\pi} \int_{-\infty}^{\infty} d\mu \frac{e^{j\mu x}}{|\alpha|} \sum_n e^{jn\mu x} \left[ |\tau_{Ai}^{(n)}| K_1(q_i^{(n)}) + |\tau_{Bi}^{(n)}| K_2(q_i^{(n)}) \right] \quad (2-47)$$

The above infinite integral may be transformed into a contour integral by closing the contour below, as shown in Figure 2-2. Since the poles  $\mu = \mu_m$  of the integrand are expected to lie in the lower half of the  $\mu$  plane, the above integral can be meaningful for  $|x| \rightarrow \infty$  only if  $x$  is taken to be negative. The integrand can then be written as the sum of residues:

$$\pi_i(x, z) = (-2\pi j/2\pi) \sum_m \text{Res}_m \quad (2-48)$$

where

$$\text{Res}_m = \text{Res}_m [e^{-j\mu|x|} \tilde{\pi}_i(\mu, x, z)] = \lambda_m E_m \exp(-j\mu_m|x|) \quad (2-49)$$

$$\lambda_m = \left[ a |\alpha| / \partial \mu \right]_{\mu=\mu_m}^{-1} \quad (2-50)$$

$$E_m = \sum_n e^{-jn|\mu_m|x} E_{mn} \quad (2-51)$$

$$E_{mn} = \left[ |\tau_{Ai}^{(n)}| K_1(q_i^{(n)}) + |\tau_{Bi}^{(n)}| K_2(q_i^{(n)}) \right]_{\mu=\mu_m} \quad (2-52)$$

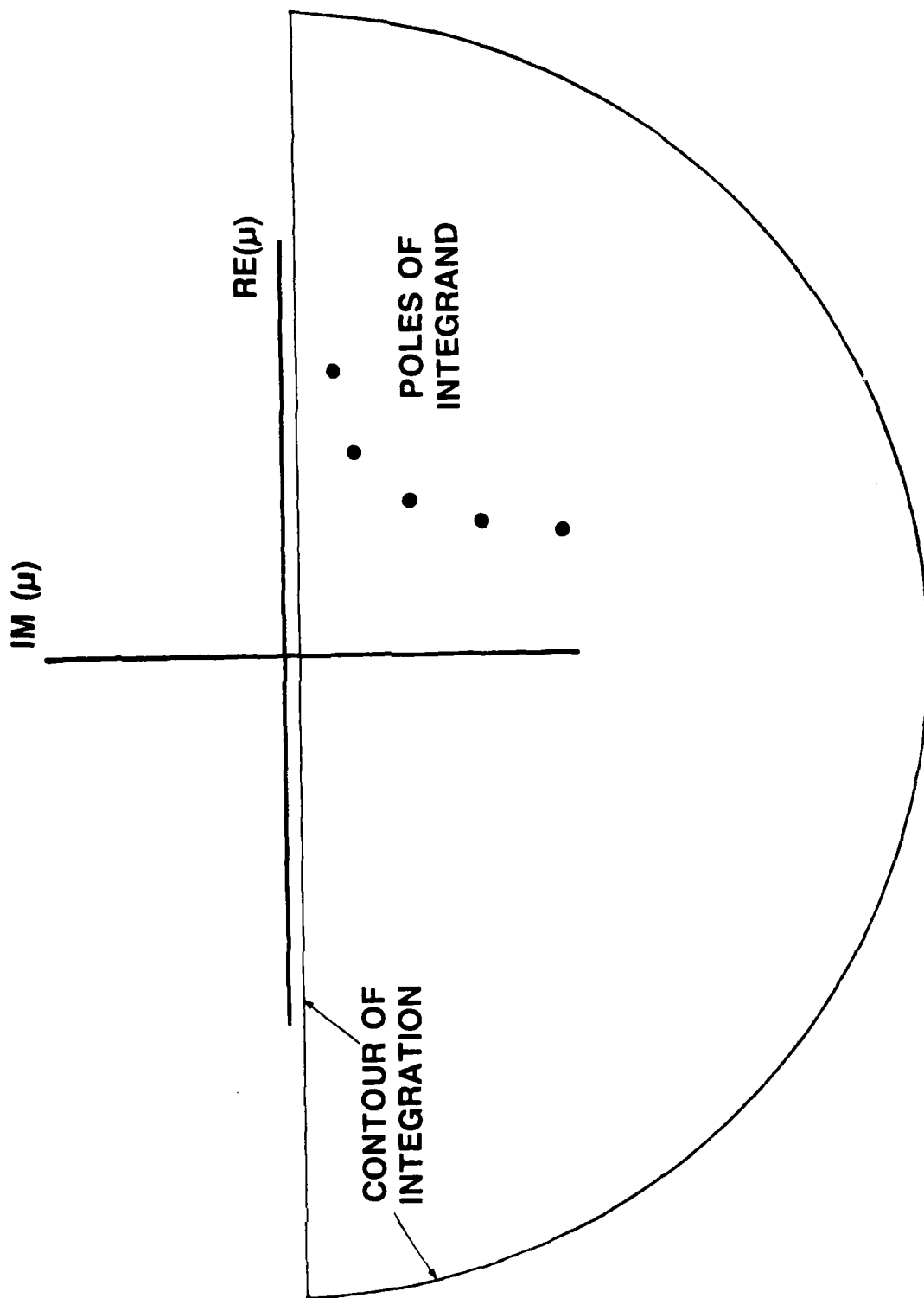


Figure 2-2. Contour for integral of Equation 2-47.

Equation 2-48, therefore, can be written

$$\begin{aligned}\Pi_i(x,z) &= -j \sum_m \lambda_m \exp[-j\mu_m |x|] \sum_n e^{-j\kappa n |x|} E_{mn} \\ &= -j \sum_m \lambda_m E_m \exp[-j\mu_m |x|]\end{aligned}\tag{2-53}$$

### SUMMARY

In Equation 2-42, the matrix of the characteristic determinant has been divided into submatrixes, with those containing the  $a_{ij}^{(n)}$  elements lying along the diagonal. By using the definitions in Equation 2-34, it is seen that the roughness, characterized by the roughness amplitude  $\epsilon$ , appears only in the rows containing the  $a_{11}^{(n)}$  and  $a_{12}^{(n)}$  terms. Since the index  $n$  labels a Floquet mode, the elements of the off-diagonal submatrixes (i.e., the elements  $U_n^{(r-n)}$ ,  $V_n^{(r-n)}$ ) are all of at least first-order in  $\epsilon$  and serve to couple together the various Floquet mode contributions.

This is seen by observing that, if all elements not contained in the diagonal submatrixes were zero, the Floquet modes may be "decoupled" from each other. Each submatrix on the diagonal would then represent an independent system of equations to determine the contribution of a Floquet mode of the problem. Because of the form of the free vector  $\beta$  in Equation 2-43, the free vector for each submatrix would then be zero except for the 0-th Floquet mode. The corresponding field coefficients (i.e.,  $A_i^{(n)}$ ,  $B_i^{(n)}$ ), therefore, would all be zero except for the 0-th Floquet mode, thereby leading to the smooth-earth solution

$$\Pi_i(x,z) = -j \sum_m \lambda_m E_{m0} \exp[-j\mu_m |x|]\tag{2-54}$$

This does not imply that eigenvalues (or zeroes of  $||\alpha||$ ) of only the 0-th order submatrix are present. Just as there are zeroes of the 0-th order submatrix, there are zeroes of the other submatrixes representing other Floquet modes. However, in the limit of zero roughness, only those modes representing the eigenvalues of the 0-th order submatrix are excited. Referring to Equation 2-52, the  $\tau_{Ai}^{(n)}$  and  $\tau_{Bi}^{(n)}$  would be non-zero only for  $n = 0$  and only for roots  $\mu = \mu_m$  of  $||\alpha||$  corresponding to the roots of the 0-th order submatrix. Therefore, the sum in Equation 2-54 is over only those eigenvalues of the 0-th order submatrix.

The locations in the complex  $\mu$ -plane of eigenvalues  $\mu_m$  of each Floquet contribution are illustrated schematically in Figure 2-3 for the case of zero roughness. Since the only difference in each submatrix is the index  $n$  of  $\mu^{(n)}$ , the set of eigenvalues for each value of  $n$  would be translated from the set of modes for  $n = 0$  by an amount  $\kappa n$  along the real axis. There is no way of associating particular eigenvalues with specific values of  $n$  when the roughness is large. When the roughness is non-zero but small, it is expected that their location in the complex plane differs only slightly from the zero roughness case so that identification between a given set of eigenvalues and a particular Floquet series element can still be made.

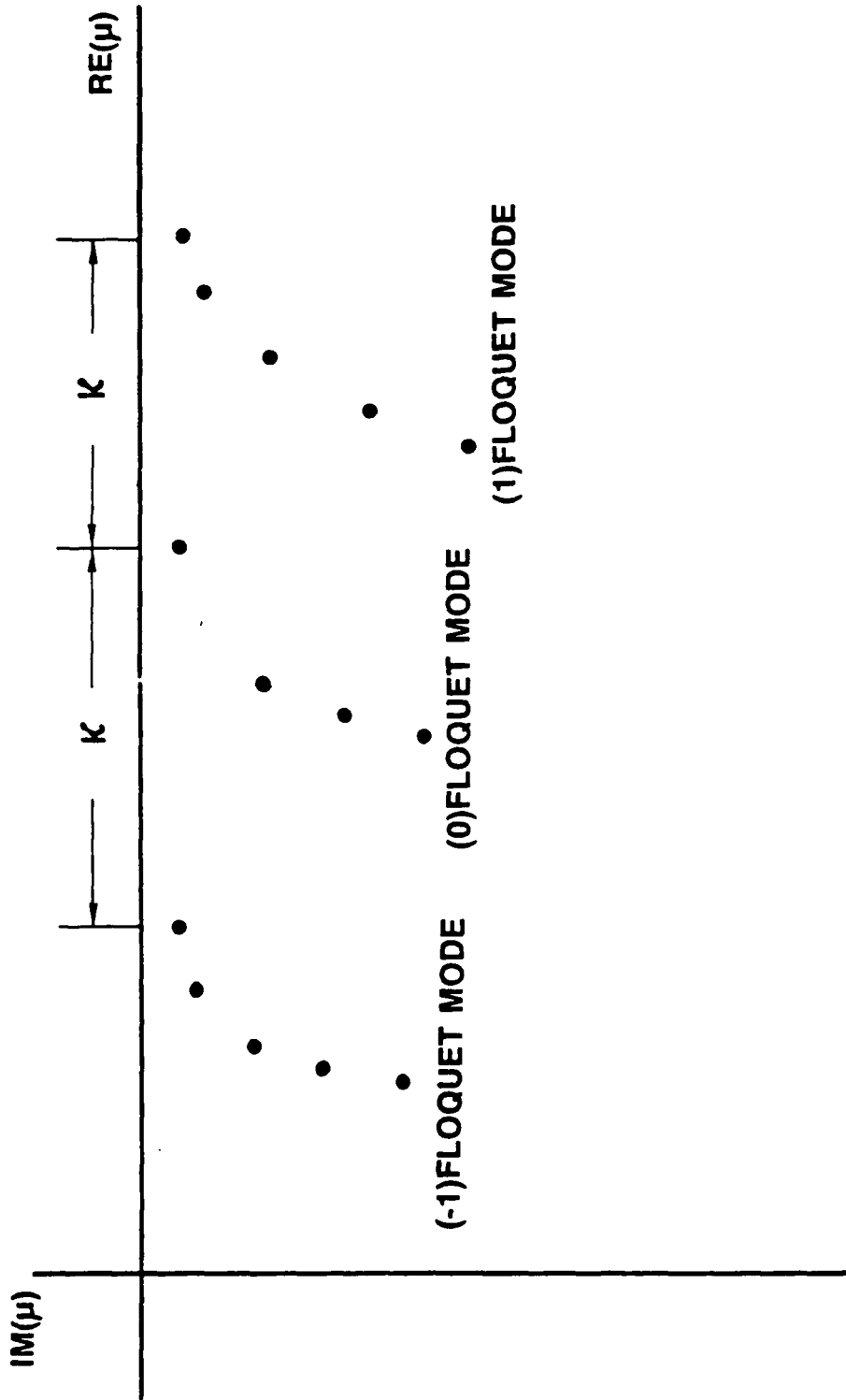


Figure 2-3. Schematic location of smooth surface eigenvalues for different Floquet contributions.

SECTION 3  
EFFECTIVE REFLECTION COEFFICIENT AND WAVEGUIDE  
MODE ATTENUATION

GENERAL

In the previous section, solutions to the electromagnetic field equations for horizontally polarized waves propagating in a duct situated over a perfectly conducting, rough earth were obtained. These solutions depend on determining eigenvalues that are the roots of an infinite determinant.

In this section, a waveguide mode formulation is used to derive an effective ground reflection coefficient. This reflection coefficient is used in the fundamental waveguide mode equation to determine the eigenvalues of a waveguide with a periodically rough boundary as a perturbation of the smooth boundary values. The roughness is found to cause attenuation in trapped modes, and this attenuation can be expressed in a simple manner. It reduces to a closed-form expression when the duct is approximated by a bilinear refractivity profile. This approach is entirely equivalent to that given in the last section but provides greater physical insight into the waveguide phenomenon.

REFLECTION COEFFICIENTS

A horizontally homogeneous atmosphere is characterized by a continuous piecewise linear refractivity profile with  $L$  sections (refer to Figure 3-1). Using Equations 2-1 and 2-2, the modified refractivity of the  $i$ -th section of the profile can be written as

$$M_i(z) \approx \frac{1}{2}[m_i^2(z) - 1] \times 10^6, \quad 1 \leq i \leq L \quad (3-1)$$

where  $m_i(z)$  is the modified index of refraction. For sinusoidal roughness, the ground surface satisfies

$$f(x) = \epsilon \sin(\kappa x + \phi) \quad (3-2)$$

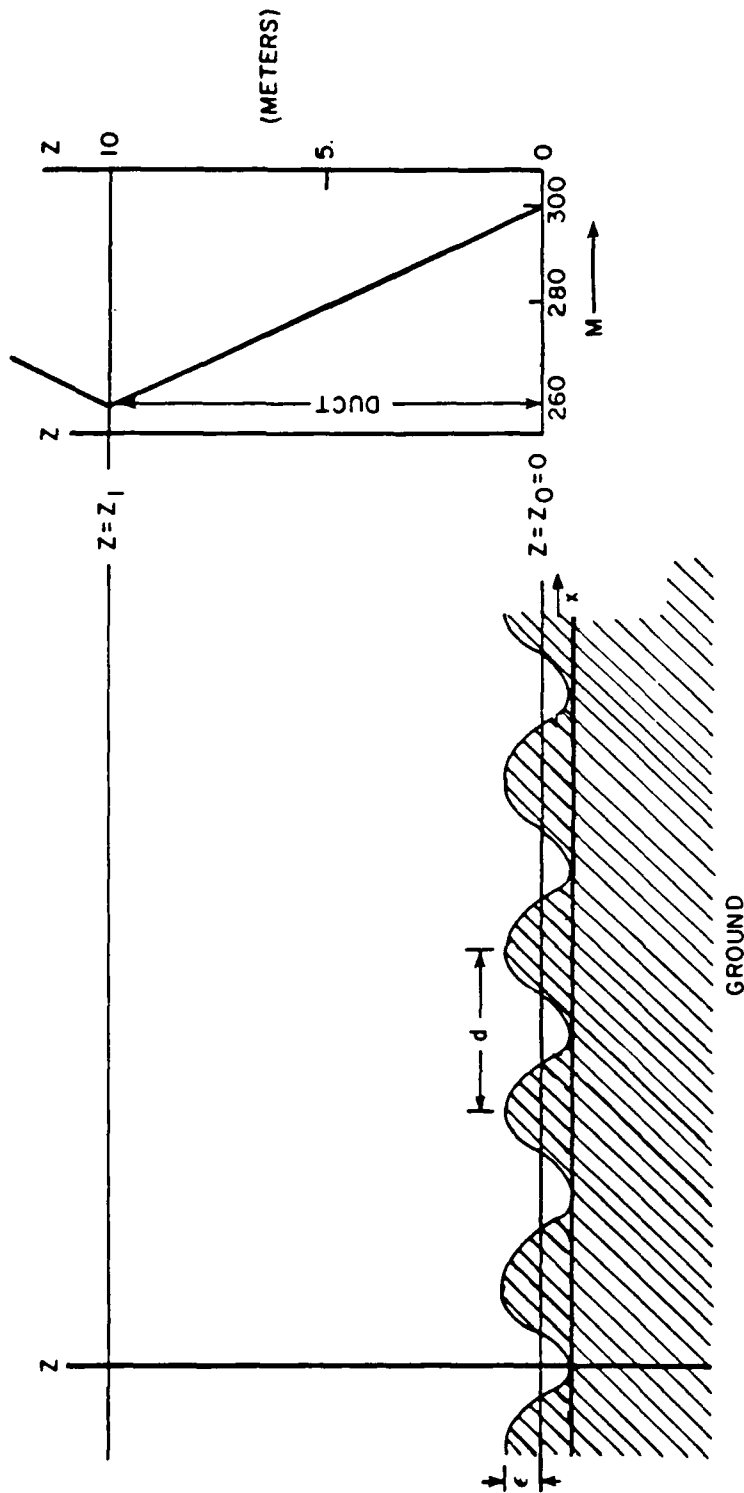


Figure 3-1. Physical model for duct calculations over sinusoidal rough earth.

where  $\kappa = 2\pi/d$  and  $d$  is the spatial period of the roughness.

Assume that the region below  $z = 0$  (see Figure 3-1) is half-space consisting of material with the same refraction index  $m_0$  as the atmosphere at  $z = 0$ , and that a plane wave characterized by  $\exp(j\mu^{(n)}x)\exp(-j\gamma^{(n)}z)$  is incident on the  $z = 0$  interface from below, where

$$\gamma^{(n)} = (k_0^2 - \mu^{(n)2})^{1/2} = k_0 \sin \theta^{(n)} \quad (3-3)$$

$\mu^{(n)} \equiv \mu + \kappa n$ ,  $k_0 = m_0 k$ ,  $\theta^{(n)}$  is the grazing angle, which may be complex, and  $n$  is a positive or negative integer. Since an  $e^{j\omega t}$  time dependence is assumed, the wave is propagating in the negative  $x$  direction, and  $\text{Re}(\mu^{(n)}) > 0$ ,  $\text{Re}(\gamma^{(n)}) > 0$ . The total field in the region  $z < 0$  then will be characterized by  $\exp(j\mu^{(n)}x) [\exp(-j\gamma^{(n)}z) + R^{(n)} \exp(j\gamma^{(n)}z)]$ , where  $R^{(n)}$  is the corresponding "upward-looking" reflection coefficient.

Now consider the case of a plane wave incident on the rough surface from above. The region above is now assumed to be homogeneous with refraction index  $m_0$ , and the incident field is characterized by  $\exp(j\mu^{(n)}x)\exp(j\gamma^{(n)}z)$ . Since the ground is periodic with wave number  $\kappa$ , there will be waves reflected in discrete directions (see Figure 3-2), so that the reflected field above the ground will have the form:

$$\sum_m (-\delta_{nm} + \bar{R}_{nm}) \exp(j\mu^{(m)}x)\exp(-j\gamma^{(m)}z) \quad (3-4)$$

where  $\delta_{nm}$  is the Kronecker delta function, and the sum is over all positive and negative  $m$ . The  $\bar{R}_{nm}$  are elements of a "downward-looking" roughness reflection matrix in which the element  $(n,m)$  represents the portion of the field which, because of the roughness, is reflected into a wave characterized by  $\mu^{(m)}$  when the incident wave is characterized by  $\mu^{(n)}$ . By expanding the

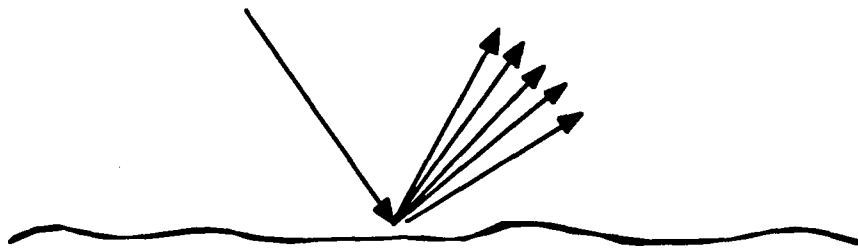


Figure 3-2. Discrete spectrum of plane wave reflection from sinusoidal rough surface.

field and the boundary in powers of the roughness amplitude  $\epsilon$  (Reference 3-1), it can be shown that, when the horizontally polarized  $\vec{E}$  vector is normal to the direction of roughness variation,

$$\bar{R}_{n,n}(\epsilon) = 1/2\epsilon^2 \gamma^{(n)} (\gamma^{(n-1)} + \gamma^{(n+1)}) + O(\epsilon^3) \quad (3-5)$$

$$\bar{R}_{n,n+1}(\epsilon) = -j \epsilon \gamma^{(n)} e^{j\phi} + O(\epsilon^2) \quad (3-6)$$

$$\bar{R}_{n,n-1}(\epsilon) = -j \epsilon \gamma^{(n)} e^{-j\phi} + O(\epsilon^2) \quad (3-7)$$

$$\bar{R}_{n,n-m}(\epsilon) = O(\epsilon^2) \quad (3-8)$$

---

3-1 Fessenden, D. E., "Space Wave Field Produced by a Horizontal Electric Dipole above a Perfectly Conducting Sinusoidal Ocean Surface," Third International Conference on Antennas and Propagation ICAP 83, 1983.

The upward- and downward-looking reflection coefficients are used in the following subsections to obtain the modes of the atmospheric waveguide.

#### WAVEGUIDE MODE EQUATION

The modes of a smooth-earth atmospheric waveguide can be thought of as discrete grazing angles  $\theta_m$ , or equivalently discrete wave numbers  $\mu_m$ , characterizing plane waves at a given altitude within the waveguide. Choosing that altitude as  $z = 0$ , each such plane wave will have the property that, after a complete cycle of reflection from the upper boundary and reflection from the lower boundary, its amplitude and phase at each value of  $x$  along  $z = 0$  will be identical to those of the original wave. This may be expressed as

$$R^{(0)}(\mu_m) \bar{R}(\mu_m) - 1 = 0 \quad (3-9)$$

where  $R^{(0)}$  is the upward-looking reflection coefficient and  $\bar{R}$  is the downward-looking reflection coefficient. For a horizontally polarized wave propagating over perfectly conducting ground,

$$\bar{R}(\mu) = -1, \text{ all } \mu \quad (3-10)$$

so that the  $\mu_m$  satisfy

$$R^{(0)}(\mu_m) = -1 \quad (3-11)$$

Although Equation 3-9 was derived on the basis of a single cycle of reflections from the upper and lower waveguide walls, the result would be identical if any number of cycles were used.

If a sinusoidal roughness is now considered, the situation is more complex, since a wave incident on the rough surface from above is reflected into an infinite set of discrete directions (see Figure 3-2). Limiting the discussion to those wave components within the propagation medium characterized by the wave number  $\mu^{(0)}$ , Equation 3-9 can be generalized to a rough-surface waveguide as

$$S(\mu_m, \delta) \equiv R^{(0)} \bar{R}(\mu^{(0)}, \delta) - 1 = 0 \quad (3-12)$$

where  $\delta$  is a small quantity characterizing the roughness,

$$\bar{R}(\mu^{(0)}, \delta) = -1 + \Delta \bar{R}(\mu^{(0)}, \delta) \quad (3-13)$$

is an effective reflection coefficient, and  $\Delta \bar{R}$  is the reflection coefficient correction due to roughness for waves characterized by  $\mu^{(0)}$ .

Some thought indicates that a component of the ground-reflected wave that is not in the specular direction, because of the assumed waveguide nature of the propagating medium, will be reflected back to the ground from the upper wall of the guide (see Figure 3-3). Upon re-reflection from the ground, another discrete spectrum of waves is obtained, including a component characterized by the original  $\mu = \mu^{(0)}$  wave number. The same process can occur after any number of ground reflections.

Referring to Equations 3-5 through 3-8, note that after a single reflection from the ground, the reflection coefficient correction for the  $\mu^{(0)}$  component of the reflected field is  $\bar{R}_{0,0}$ . This corresponds to wave BHE in Figure 3-3. After an additional cycle, there is a reflection coefficient correction contribution in the  $\mu^{(0)}$  direction due to a wave that was first reflected into a  $\mu^{(m)}$  direction and then reflected back into a  $\mu^{(0)}$  direction (such as BGCJ in Figure 3-3). This contribution is

$$\bar{R}_{0,m} [R^{(m)} \bar{R}_{m,0}] = \bar{R}_{0,m} \bar{R}_{m,0} R^{(m)}.$$

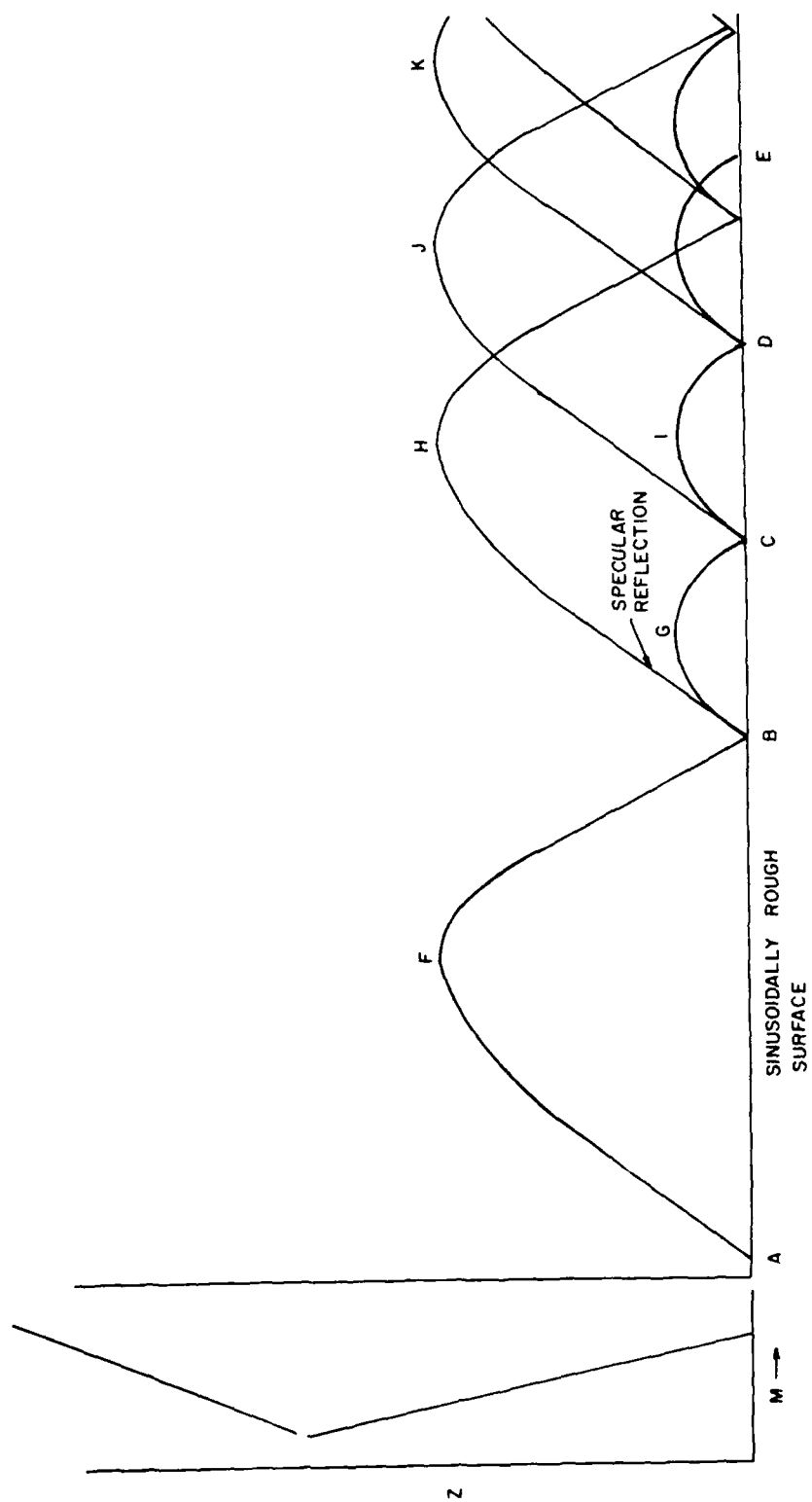


Figure 3-3. Mode scattering out of and into the (0) specular direction.

If the reflection coefficient correction contributions are to be of order  $\epsilon^2$ , it is seen from Equations 3-6 through 3-8 that  $m$  can take on only the values of  $\pm 1$ . With this limitation, the contribution to  $\Delta \bar{R}$  after an additional cycle would occur as a result of the original  $\mu^{(0)}$  wave being scattered into a  $\mu^{(m)}$  wave after the first reflection, scattered specularly into a  $\mu^{(m)}$  wave after the second reflection, and scattered back into a  $\mu^{(0)}$  wave after the third reflection. This contribution to the reflection coefficient correction is

$$\bar{R}_{0,m} [R^{(m)} (-1 + \bar{R}_{m,m})] [R^{(m)} \bar{R}_{m,0}] \approx \bar{R}_{0,m} \bar{R}_{m,0} (-R^{(m)2}) + O(\epsilon^3), m = \pm 1$$

This corresponds to BGCIDK in the figure. In general, after  $N + 1$  cycles, the reflection coefficient correction contribution is

$$\bar{R}_{0,m} \bar{R}_{m,0} (-R^{(m)})^N, m = \pm 1.$$

Summing all these contributions for  $m = -1$  and  $m = 1$  yields

$$\Delta \bar{R} = \bar{R}_{0,0} - \bar{R}_{0,-1} \bar{R}_{-1,0} \sum_i (-R^{(-1)})^i - \bar{R}_{0,1} \bar{R}_{1,0} \sum_i (-R^{(1)})^i \tag{3-14}$$

where the sums are over all integers  $i \geq 1$ . Equation 3-14 can be considered an expansion of  $\Delta \bar{R}$  for small values of  $|R^{(-1)}|$  and  $|R^{(1)}|$ . As  $R^{(-1)}$  and  $R^{(1)}$  increase in magnitude,  $\Delta \bar{R}$  contains more of an interaction between the ground and the propagation medium. In such a case, use of  $\bar{R}_{0,0}$  alone (which, like  $\Delta \bar{R}$  in Equation 3-1, describes only the energy scattered out of the specular direction) is insufficient to compute  $\Delta \bar{R}$ .

Substituting Equations 3-5 through 3-7 in Equation 3-14 yields

$$\Delta \bar{R} = -2\gamma^{(0)} \left[ \gamma^{(-1)} \frac{R^{(-1)} - 1}{R^{(-1)} + 1} + \gamma^{(1)} \frac{R^{(1)} - 1}{R^{(1)} + 1} \right] \frac{\epsilon^2}{4} \tag{3-15}$$

where the identity  $\sum_i (-R)^i = -R/(1+R)$  was used. From Equation 3-15 it is clear that  $\bar{\Delta R}$  is proportional to  $\epsilon^2$ . For future convenience,  $\delta$  will be defined as  $\frac{1}{4} \epsilon^2$ . The relationships in Equations 3-13 and 3-14 may be used in Equations 3-12 to obtain the eigenvalues  $\mu_m$ .

### EIGENVALUE PERTURBATIONS

A separate numerical search for the eigenvalues, or roots, of Equation 3-12 is required for each value of  $\epsilon$  or  $d$ . This eigenvalue search is extremely time consuming. A method is now described that, to the same degree of accuracy, permits the rapid calculation of the  $\mu_m(\epsilon)$  for any set of  $(\epsilon, d)$ , once the  $\mu_m(0)$  have been found.

For a small roughness amplitude  $\epsilon$ , the eigenvalues can be expanded as

$$\mu_m(\delta) = \mu_m(0) + \Delta\mu_m \quad (3-16)$$

where

$$\Delta\mu_m = d\mu_m(0)/d\delta \delta \quad (3-17)$$

is the amount by which the  $m$ -th eigenvalue is changed as a result of the roughness through the process of scattering energy out of and back into the specular direction. Now,

$$dS = S_\mu d\mu + S_\delta d\delta \quad (3-18)$$

where the subscripts  $\mu$  and  $\delta$  indicate partial differentiation, and the partial derivatives may be evaluated at  $\mu = \mu_m(0)$ ,  $\delta = 0$ . Choosing  $d\mu$  and  $d\delta$  such that  $\mu$  remains an eigenvalue requires that  $dS = 0$ . Therefore,

$$d\mu_m(0)/d\delta = -S_\delta/S_\mu \quad (3-19)$$

Substituting this in Equation 3-17 and using Equation 3-12 results in

$$\Delta\mu_m = -\Delta\bar{R}(\mu_m(0), \delta) / R_\mu^{(0)}(\mu_m(0)) \quad (3-20)$$

where Equations 3-10 and 3-11 were used.

Numerical calculations indicate that for the  $\mu_m$  representing the least attenuated modes of propagation,

$$\mu_m/k_0 \approx 1 \quad (3-21)$$

and that

$$|R^{(1)}(\mu_m)| \gg 1, \quad |R^{(-1)}(\mu_m)| \ll 1 \quad (3-22)$$

when

$$\kappa/k_0 > [1 - (\mu_m/k_0)^2]^{1/2} \sim 10^{-4} \quad (3-23)$$

From Equation 3-15, this leads to

$$\Delta\bar{R} \approx \frac{1}{2} \gamma^{(0)} (\gamma^{(-1)} - \gamma^{(1)}) \epsilon^2 \quad (3-24)$$

Using Equation 3-21 it may be shown that for  $\kappa/k_0$  not very large,

$$\gamma^{(\pm 1)} \approx k_0 [(\kappa/k_0) (\mp 2 - \kappa/k_0)]^{1/2} \quad (3-25)$$

Then, using Equation 3-3,

$$\Delta \bar{R} \approx \frac{1}{2} [(2 - \lambda/d)^{\frac{1}{2}} - j(2 + \lambda/d)^{\frac{1}{2}}] [\sin \theta^{(0)} k_0^2 (\lambda/d)^{\frac{1}{2}} \epsilon^2] \quad (3-26)$$

where  $\lambda = 2\pi/k_0$ . The first factor in brackets on the right-hand side is of order unity for all  $\lambda/d \leq 1$ . The second factor represents the small quantity in which  $\bar{R}$  is being expanded. Comparing it with the square of the Rayleigh factor of Equation 3-1, it is seen that  $\sin^2 \theta$  in the latter is replaced here by  $\sin \theta$  times  $(\lambda/d)^{\frac{1}{2}}$ . For most cases of interest, the Rayleigh factor will be smaller. It should not be surprising, then, if common situations arise in which additional terms in the expansion of Equation 3-16 are required.

Using Equation 3-26 in Equation 3-20 yields

$$\Delta \mu_m \approx -2 [(2 - \lambda/d)^{\frac{1}{2}} - j(2 + \lambda/d)^{\frac{1}{2}}] [\sin \theta^{(0)} / R_\mu^{(0)}] [k_0^2 (\lambda/d)^{\frac{1}{2}}] \delta \quad (3-27)$$

### TRAPPED MODES

The ratio  $\sin \theta^{(0)} / R_\mu^{(0)}$  in Equation 3-27 depends on the eigenvalue  $\mu_m$ . For trapped modes, which are identified by Marcus and Stuart (Reference 1-4),

$$\text{Im}(\sin \theta^{(0)}) \approx 0 \quad (3-28)$$

This ratio can be obtained from the phase integral approximation (Reference 1-5) according to which

$$R^{(0)} = e^{-j(\psi - \frac{1}{2}\pi)} \quad (3-29)$$

where

$$\psi = \psi(\theta) = 2k \int_0^{\xi} [m(z)^2 - c^2]^{\frac{1}{2}} dz \quad (3-30)$$

$$C = m_0 \cos \theta \quad (3-31)$$

and  $z = \xi(\theta)$  is the root of  $m(z)^2 - C^2 = 0$  and is the height at which a ray with grazing angle  $\theta$  at  $z = 0$  will experience a turning point. From Equation 3-11, the eigenvalues  $\theta = \theta_m$  satisfy

$$\psi(\theta) = (2m + 3/2)\pi, \quad m = \text{integer} \quad (3-32)$$

From Equation 3-3,  $\mu_m = k_0 \cos \theta$  so that

$$R_\mu^{(0)} = k_0^{-1} \partial R^{(0)} / \partial \cos \theta = -k_0^{-1} \cot \theta \partial R^{(0)} / \partial \sin \theta \quad (3-33)$$

which should be evaluated at  $\theta = \theta_m$ . Equations 3-29 through 3-33 can be evaluated numerically for any desired surface duct profile, or can be evaluated in closed form for the piecewise linear, two-layer profile illustrated in Figure 3-1. For this case, and for all  $m$ ,

$$\sin \theta_m / R_\mu^{(0)} = -\frac{1}{4} j \tan \alpha_1 \quad (3-34)$$

thereby providing a closed form expression for  $\Delta\mu_m$  in Equation 3-27:

$$\Delta\mu_m = \frac{1}{2} [(2 + \lambda/d)^{\frac{1}{2}} + j(2 - \lambda/d)^{\frac{1}{2}}] \tan \alpha_1 k_0^2 (\lambda/d)^{\frac{1}{2}} \delta \quad (3-35)$$

From Equations 3-28 through 3-33, it can be shown that for trapped modes,

$$\text{Re}(R_\mu^{(0)}) \approx 0 \quad (3-36)$$

Using Equations 3-28 and 3-36 in Equation 3-27 yields

$$\text{Im}(\Delta\mu_m) = 2(2 - \lambda/d)^{\frac{1}{2}} [j \sin \theta^{(0)} / R_\mu^{(0)}] [k_0^2 (\lambda/d)^{\frac{1}{2}}] \delta,$$

$$d > \lambda/2, \text{ trapped modes} \quad (3-37)$$

PROPAGATION LOSS RATE

The contribution of each waveguide mode to the total field has a dependence on the distance  $|x|$  given by  $\exp[-j\mu_m(\epsilon) |x|]$ , where  $|x|$  can increase to large values (References 1-3 and 1-4). If  $\Delta\mu_m$  has a non-zero imaginary part, the exponential decay factor of  $\exp[-j \Delta\mu_m |x|]$  can produce a large effect on the field that varies with distance. The change  $L_m$  in propagation loss for the  $m$ -th mode over that which is experienced over smooth earth is

$$L_m = -20 \log_{10} \{ \exp[\text{Im}(\Delta\mu_m) |x|] \} = -8.68589 \text{Im}(\Delta\mu_m) |x| \quad (\text{dB}) \quad (3-38)$$

It is convenient to define the rate of loss of the  $m$ -th mode due to roughness as

$$L_{Rm} = L_m / |x| = -8.68589 \text{Im}(\Delta\mu_m) \quad (\text{dB/km}) \quad (3-39)$$

where  $\Delta\mu$  is in units of  $\text{km}^{-1}$ .

The fact that  $\Delta\mu_m$  is proportional to  $\epsilon^2$  permits a definition of roughness loss per unit distance per square of roughness amplitude:

$$L_{Sm} = 10^{-6} L_{Rm} / \epsilon^2 \quad (3-40)$$

where  $\epsilon$  is in meters.

Using Equation 3-37 in Equations 3-39 and 3-40 yields

$$L_{Sm} \approx 8.68589 (10^{-6}) k_0^2 \sin \theta_m [\lambda/d (2 - \lambda/d)]^{1/2} / [2jR_\mu^{(0)}],$$

$$(dB/km/m^2), d > \lambda/2, \text{ trapped modes} \quad (3-41)$$

and using Equation 3-34 in Equation 3-41 yields

$$L_{Sm} \approx 1.0857 (10^{-6}) |\tan \alpha_1| k_0^2 (\lambda/d)^{1/2} (2 - \lambda/d)^{1/2} (dB/km/m^2),$$

$$d > \lambda/2, \text{ trapped modes, bilinear profile} \quad (3-42)$$

where  $\lambda$  and  $d$  are in the same units, and the  $k_0$ ,  $\mu$ , and  $\tan \alpha_1$  are in units of  $km^{-1}$ .  $L_{Sm}$  as given in Equation 3-42 is always positive, thereby indicating the detrimental effect that roughness has on the ability of the trapped modes to propagate unattenuated.

It is interesting to note that if the only contribution to the reflection coefficient correction came from energy scattered out of the specular direction, then  $\Delta \bar{R} = \bar{R}_{0,0}$ . Comparing Equations 3-5 and 3-24, this is tantamount to replacing  $-\gamma^{(1)}$  by  $\gamma^{(1)}$  in Equation 3-24. Since only the real part of  $\Delta \bar{R}$  enters the expression of  $L_{Sm}$  for trapped modes, Equation 3-41 would be obtained for this case as well. It should be emphasized that  $L_{Sm}$  is identical for the partial scattering and the full scattering cases only when the modes are fully trapped. Furthermore, though the loss rate with distance may be the same for these modes, the roughness effect on the fields would be different since  $\Delta \bar{R}$  also affects the phase of  $\exp(-j\Delta\mu_m|x|)$ .

To demonstrate the effect of roughness on the modes of propagation, a plot is provided in Figure 3-4 of  $L_{Sm}$  as a function of the roughness spatial period  $d$  for the two trapped modes obtained using the surface duct refractivity provided in Figure 3-1.  $L_{Sm}$  in these plots was calculated from Equation 3-42 using a frequency of 6.814 GHz, corresponding to  $\lambda = 4.4$  cm.

For these trapped modes,  $L_{Sm}$  exhibits relatively large values in the vicinity of  $d = \lambda$ . The maximum value occurs at the value of  $\kappa$  at which  $dL_{Sm}/d\kappa = 0$ , which from Equation 3-42, is seen to occur at  $d \approx \lambda$ .

#### SUMMARY

A method for obtaining the effect of sinusoidal roughness with a small amplitude on the waveguide eigenvalues of horizontally polarized radio waves propagating in a horizontally homogeneous atmosphere has been described. The method is based on the fundamental waveguide mode equation and utilizes an eigenvalue perturbation scheme. The eigenvalue perturbations, as well as roughness loss rates, are expressed in terms of reflection coefficients that consider energy scattered out of as well as into the specular direction.

A closed-form expression is provided for the roughness attenuation rate of trapped modes in an atmosphere approximated by a bilinear refractivity profile. This attenuation rate was found to be largest when the propagation wave length and the surface roughness spatial period are close in value.

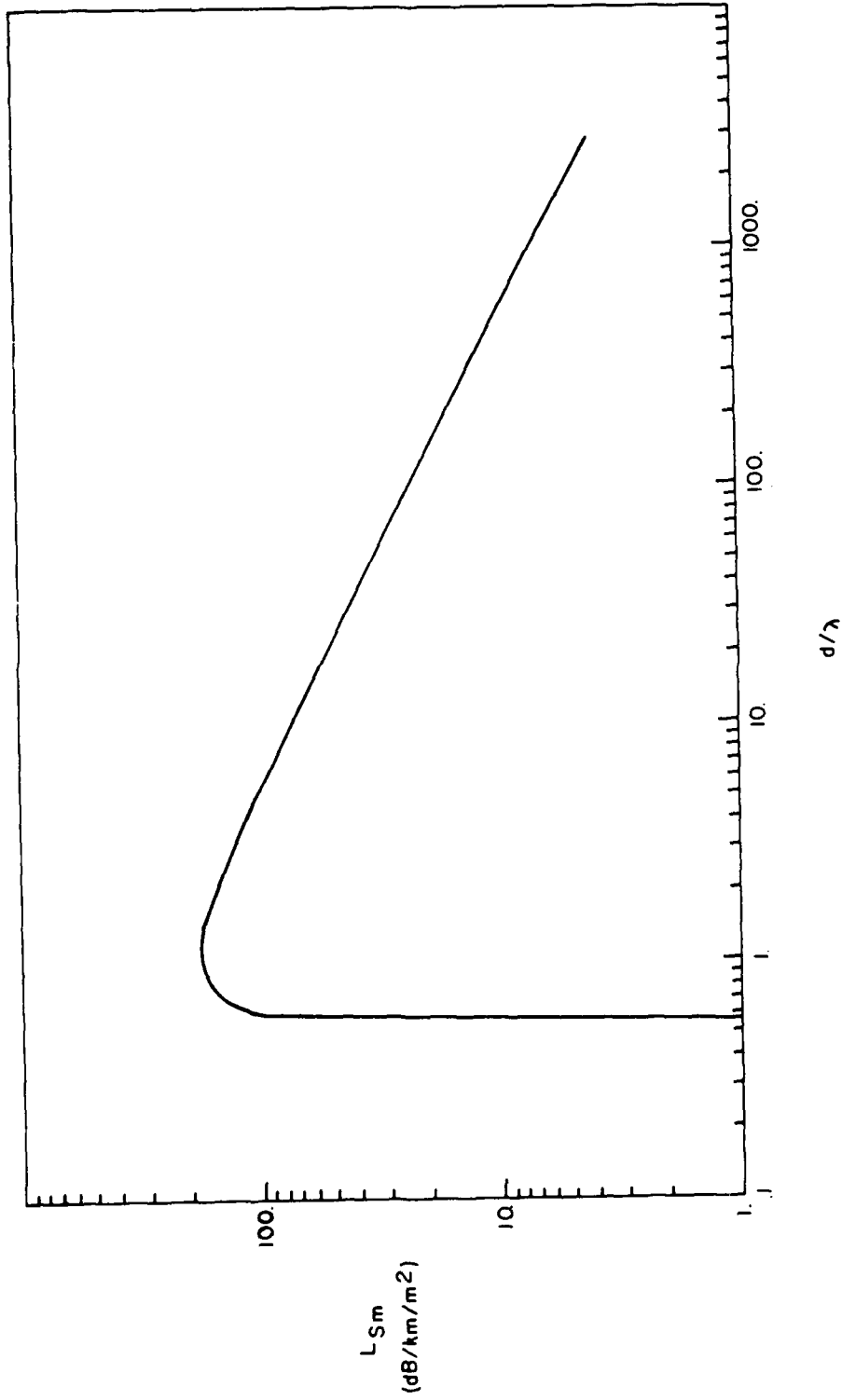


Figure 3-4. Roughness loss rate  $L_{Sm}$  as a function of  $d/\lambda$  for trapped modes of Figure 3-1,  $\lambda = 4.4$  cm.

SECTION 4  
SOLUTION FOR SINUSOIDAL ROUGHNESS

GENERAL

The general approach to the solution of the basic equations involving electromagnetic wave propagation in a surface duct over a sinusoidal rough earth was presented in Section 2. This consisted of a waveguide mode method formulated for determining the field strength over a slightly rough earth. The eigenvalues of the waveguide formulation were found as roots of an infinite determinant that reduces to the smooth-earth eigenvalues as the ground roughness  $\epsilon$  approaches zero.

In this section the matrix is written in a form such that, when the roughness  $\epsilon$  approaches zero, the determinant becomes a product of subdeterminants, each representing a Floquet mode of propagation. As in the last section, the roughness is assumed to be sinusoidal, given by Equation 3-2.

For the case of  $L = 2$ , and including for demonstration purposes only the central  $9 \times 9$  elements,

$$\alpha = \begin{bmatrix}
 a_{11}^{(-1)} & a_{12}^{(-1)} & & b_1^{(0)} & b_2^{(0)} & c_1^{(1)} & c_2^{(1)} \\
 a_{21}^{(-1)} & a_{22}^{(-1)} & a_{23}^{(-1)} & & & & \\
 a_{31}^{(-1)} & a_{32}^{(-1)} & a_{33}^{(-1)} & & & & \\
 d_1^{(-1)} & d_2^{(-1)} & & a_{11}^{(0)} & a_{12}^{(0)} & b_1^{(1)} & b_2^{(1)} \\
 & & & a_{21}^{(0)} & a_{22}^{(0)} & a_{23}^{(0)} & \\
 & & & a_{31}^{(0)} & a_{32}^{(0)} & a_{33}^{(0)} & \\
 e_1^{(-1)} & e_2^{(-1)} & & d_1^{(0)} & d_2^{(0)} & a_{11}^{(1)} & a_{12}^{(1)} \\
 & & & & & a_{21}^{(1)} & a_{22}^{(1)} & a_{23}^{(1)} \\
 & & & & & a_{31}^{(1)} & a_{32}^{(1)} & a_{33}^{(1)}
 \end{bmatrix} \quad (4-1)$$

where

$$a_{2i}^{(n)} = K_i(q_{11}^{(n)}), \quad a_{3i}^{(n)} = K_i'(q_{11}^{(n)}), \quad i = 1, 2; \quad (4-2)$$

$$a_{23}^{(n)} = -K_2(q_{21}^{(n)}), \quad a_{33}^{(n)} = -K_2'(q_{21}^{(n)})q_2'/q_1', \quad \text{all } n$$

$$\begin{aligned}
a_{1i}^{(n)} &= K_i(q_{10}^{(n)}) [1 - \frac{1}{4} \epsilon^2 \gamma^{(n)2}], \\
e_i^{(n)} &= -(\epsilon^2/8) K_i(q_{10}^{(n)}) \gamma^{(n)2} e^{2j\phi}, \\
c_i^{(n)} &= -(\epsilon^2/8) K_i(q_{10}^{(n)}) \gamma^{(n)2} e^{-2j\phi}, \\
d_i^{(n)} &= \frac{1}{2}\epsilon K_i'(q_{10}^{(n)}) q_1' e^{j\phi}, \\
b_i^{(n)} &= \frac{1}{2}\epsilon K_i'(q_{10}^{(n)}) q_1' e^{-j\phi}, \quad i = 1, 2; \text{ all } n.
\end{aligned} \tag{4-3}$$

The  $K_1(q)$  and  $K_2(q)$  are linear combinations of modified Hankel functions of order one-third (Reference 2-1).

$$q_{ij}^{(n)} \equiv q_i^{(n)}(z_j) = (k/|\tan \alpha_i|)^{2/3} [m_i^2(z_j) - \mu^{(n)2}/k^2] \tag{4-4}$$

$$\mu^{(n)} \equiv \mu + \kappa n \tag{4-5}$$

$$\gamma^{(n)2} = k^2 m_0^2 - \mu^{(n)2} \tag{4-6}$$

$z_j$  is the upper boundary of the  $j$ -th atmospheric layer,  $z_0 = 0$ ,  $m_0 = m_1(0)$ , and primes denote differentiation with respect to the argument. The superscript  $(n)$  denotes the index of a Floquet mode.

It has been shown that in practical problems, the "power sum" expression

$$\Pi_i(x, z; \epsilon) = \left\{ \sum_m |\lambda_m \exp[-j\mu_m(\epsilon)|x|] \sum_n e^{-j\kappa n|x|} |E_{mn}|^2 \right\}^{1/2} \tag{4-7}$$

often provides more accurate predictions of the duct field relative to free space (Reference 1-3).

EQUIVALENT ZERO MODE MATRIX

When  $\epsilon$  approaches 0, the determinant  $||\alpha||$  reduces to a product of subdeterminants, each representing a Floquet mode of the propagation, and  $E_{mn} = 0$  except for  $n = 0$ . The discussion below concentrates on the effect of the roughness on the 0-th Floquet series element and on the contribution of that element to the total field. That is, when the roughness is small, the  $\mu_m(\epsilon)$  may then be used to obtain the  $E_{m0}[\mu_m(\epsilon), z, z_T; \epsilon]$  and  $\lambda_m[\mu_m(\epsilon); \epsilon]$  so that the  $n = 0$  contribution to  $\Pi_i(x, z; \epsilon)$  may be computed.

The  $\mu_m$  are the roots of  $||\alpha||$ . Referring to the infinite order matrix form, Equations 4-1 and 4-3 may be used to write, to second order in  $\epsilon$ ,

$$||\alpha|| = \left[ \prod_n D^{(n)}(\epsilon) \right] \left\{ 1 - \delta \sum_n \left[ (D_a^{(n)}/D^{(n)}) (D_a^{(n+1)}/D^{(n+1)}) \right] \right\} \tag{4-8}$$

where  $\delta \equiv \frac{1}{4}\epsilon^2$ , and

$$D^{(n)}(\epsilon) = \begin{vmatrix} a_{11}^{(n)}(\epsilon) & a_{12}^{(n)}(\epsilon) & \\ a_{21}^{(n)} & a_{22}^{(n)} & a_{23}^{(n)} \\ a_{31}^{(n)} & a_{32}^{(n)} & a_{33}^{(n)} \end{vmatrix} \tag{4-9}$$

$$D_a^{(n)} = \begin{vmatrix} b_{11}^{(n)} & b_{12}^{(n)} & \\ a_{21}^{(n)} & a_{22}^{(n)} & a_{23}^{(n)} \\ a_{31}^{(n)} & a_{32}^{(n)} & a_{33}^{(n)} \end{vmatrix} \tag{4-10}$$

$$b_{11}^{(n)} = K_1'(q_{10}^{(n)})q_1', \quad b_{12}^{(n)} = K_2'(q_{10}^{(n)})q_1' \quad (4-11)$$

and the product and sum in Equation 4-8 are over all  $n$ . Using the first expression in Equation 4-3,

$$\left[ \prod_n D^{(n)}(\epsilon) \right] = \left[ \prod_n D^{(n)}(0) \right] \left[ 1 - \delta \sum_n \gamma^{(n)2} \right] \quad (4-12)$$

so that Equation 4-8 may be written

$$||\alpha|| = \prod_n S^{(n)} \quad (4-13)$$

where

$$S^{(n)} = [1 - \delta \gamma^{(n)2}] \{ D^{(n)} - \delta D_a^{(n)} [D_a^{(n+1)}/D^{(n+1)}] \}, \quad n > 0 \quad (4-14)$$

$$S^{(0)} = [1 - \delta \gamma^{(0)2}] \{ D^{(0)} - \delta D_a^{(0)} [D_a^{(1)}/D^{(1)} + D_a^{(-1)}/D^{(-1)}] \} \quad (4-15)$$

$$S^{(n)} = [1 - \delta \gamma^{(n)2}] \{D^{(n)} - \delta D_a^{(n)} [D_a^{(n-1)}/D^{(n-1)}]\}, n < 0$$

(4-16)

and all the  $D^{(n)}$  determinants are evaluated at  $\epsilon = 0$ . Equations 4-14 through 4-16 are valid as long as the denominators are finite.

The eigenvalues corresponding to the  $n = 0$  Floquet mode, therefore, will be the roots  $\mu = \mu_m(\epsilon)$  of  $S^{(0)}$ . But determination of these roots is equivalent to determining the roots of the determinant of a matrix similar in form to that of Equation 4-9 with the substitution

$$a_{1i} \rightarrow K_1' - (j \tilde{\gamma} K_i/q') \quad (4-17)$$

$$\tilde{\gamma} = \{\delta j [D_a^{(1)}/D^{(1)} + D_a^{(-1)}/D^{(-1)}]\}^{-1} \quad (4-18)$$

where multiplication by the constant  $[1 - \delta \gamma^{(0)2}]^{-1}$  was permitted under the assumption that the source is not located in the lowest atmospheric layer. The matrix in Equation 4-9 with the substitution in Equation 4-17 will be referred to as the "equivalent matrix" for propagation over rough earth and is identical in form to the characteristic matrix for smooth-earth propagation (Reference 1-3).  $\tilde{\gamma}$  can then be interpreted as the effective propagation constant in the ground, and the effective reflection coefficient is given by

$$\bar{R} = (\gamma^{(0)} - \tilde{\gamma})/(\gamma^{(0)} + \tilde{\gamma}) = -1 + \Delta\bar{R} \quad (4-19)$$

where

$$\Delta \bar{R} \approx 2 j \delta \gamma^{(0)} [D_a^{(1)}/D^{(1)} + D_a^{(-1)}/D^{(-1)}] \quad (4-20)$$

Since Equation 4-19 represents an expansion of  $\bar{R}$  about  $\bar{R} = -1$ , it is expected to be valid when  $\Delta \bar{R}$  is small relative to unity.

The equivalent matrix can be used to determine all field contributions of the 0-th order Floquet mode. It cannot be used to obtain the contributions from other Floquet modes that correspond to the 0-th mode eigenvalues; this will remain a goal of future study.

Using a rough-earth version of the fundamental waveguide mode equation, it has been shown that

$$\Delta \bar{R} = -\gamma^{(0)} \left[ \gamma^{(-1)} \left( \frac{R^{(-1)} - 1}{R^{(-1)} + 1} \right) + \gamma^{(1)} \left( \frac{R^{(1)} - 1}{R^{(1)} + 1} \right) \right] \frac{\epsilon}{2} \quad (4-21)$$

where  $R^{(n)}$  is the reflection coefficient "looking upward" from below the rough surface. That is, if the region below  $z = 0$  (see Figure 4-1) is replaced by material with the same refraction index  $m_0$  as the atmosphere  $z = 0$ , and if a plane wave characterized by  $\exp(j\mu^{(n)}x)\exp(-j\gamma^{(n)}z)$  is incident on the  $z = 0$  interface from below, then the total field in the region  $z < 0$  will be given by  $\exp(j\mu^{(n)}x) [\exp(-j\gamma^{(n)}z) + R^{(n)}\exp(j\gamma^{(n)}z)]$ . Equations 4-20 and 4-21 can be shown to be identical by noting that

$$R^{(n)} = \frac{-j \gamma^{(n)} D^{(n)}(0) - D_a^{(n)}}{-j \gamma^{(n)} D^{(n)}(0) + D_a^{(n)}} \quad (4-22)$$

which can be obtained by solving a linear system of equations expressing the continuity of the Hertz potential and its normal derivative at the ground and at each atmospheric layer interface.

The reflection coefficient correction in Equation 4-21 includes energy scattered out of, as well as into, the specular direction. If only energy scattered out of the specular direction were included, then

$$\Delta \bar{R} = \gamma^{(0)} (\gamma^{(-1)} + \gamma^{(1)}) \epsilon^2 / 2 \quad (\text{partial scattering}) \quad (4-23)$$

#### EIGENVALUE PERTURBATIONS AND PROPAGATION LOSS RATES

If the above equivalent matrix is used, a separate eigenvalue search is required for each value of  $\epsilon$  or  $d$ . This eigenvalue search is extremely time-consuming. An eigenvalue perturbation method, therefore, will be utilized that, to the same degree of accuracy, will permit the rapid calculation of the  $\mu_m(\epsilon)$  for any set of  $(\epsilon, d)$ , once the  $\mu_m(0)$  has been found.

For a small roughness amplitude  $\epsilon$ , the eigenvalues of  $\mu = \mu_m(\epsilon)$ , corresponding to the 0-th order Floquet mode, satisfy  $S^{(0)}(\mu, \delta) = 0$  and may be expanded as

$$\mu_m(\delta) = \mu_m(0) + \Delta \mu_m \quad (4-24)$$

where (Reference 1-10)

$$\Delta\mu_m = -S_\delta^{(0)}/S_\mu^{(0)} \delta \quad (4-25)$$

Using Equation 4-15 with

$$D^{(0)}(0) = 0 \text{ when } \mu = \mu_m(0) \quad (4-26)$$

in Equation 4-25 yields

$$\Delta\mu_m = J(\mu_m, \kappa) \epsilon^2 \quad (4-27)$$

where

$$J(\mu_m, \kappa) = [D_a^{(0)} / (4 D_\mu^{(0)})] [D_a^{(-1)}/D^{(-1)} + D_a^{(1)}/D^{(1)}] \quad (4-28)$$

Each of the determinants in this equation is evaluated at  $\mu = \mu_m(0)$ ,  $\delta = \epsilon = 0$ . The  $\mu_m(\epsilon)$  resulting from the use of Equation 4-27 with Equation 4-24 can then be used in the equivalent matrix to obtain  $\lambda_m$  and  $E_{m0}$  in Equation 2-53. Thus, once the smooth-earth eigenvalues have been found, the field contributions of the 0-th Floquet mode can be determined for any combination of  $\epsilon$  and  $d$  without performing a time-consuming numerical search for the new eigenvalues. The accuracy of the eigenvalues obtained using this perturbation method is the same as that obtained using an eigenvalue search of the determinant of the equivalent matrix, since this determinant is itself the result of an expansion in the same small quantity.

Using the fundamental waveguide mode equation, it was shown that (Reference 1-10)

$$\Delta\mu_m = -\Delta\bar{R} / R_\mu^{(0)} \quad (4-29)$$

where the subscript  $\mu$  indicates partial differentiation with respect to  $\mu$ . From Equations 4-22 and 4-26, it may be seen that, when  $\mu = \mu_m(0)$ ,

$$R_\mu^{(0)} = -2j\gamma^{(0)} D_\mu^{(0)}(0) / D_a^{(0)} \quad (4-30)$$

The consistency of Equations 4-29 and 4-27 is demonstrated by substituting Equations 4-20 and 4-30 into Equation 4-29. Thus, the eigenvalue perturbation form of Equation 4-27 considers scattering both out of and into the specular direction. If only scattering out of the specular direction were to be considered, Equations 4-23 and 4-30 may be used in Equation 4-29 to yield

$$\Delta\mu_m = j [D_a^{(0)}(0) / 4D_\mu^{(0)}] (\gamma^{(-1)} + \gamma^{(1)}) \epsilon^2 \quad (\text{partial scattering}) \quad (4-31)$$

The rate of loss due to roughness of the  $m$ -th mode along the propagation direction is defined by

$$L_{Rm} = -8.68589 \operatorname{Im}(\Delta\mu_m) \quad (\text{dB/km}) \quad (4-32)$$

where  $\Delta\mu$  is in units of  $\text{km}^{-1}$ . The fact that  $\Delta\mu_m$  is proportional to  $\epsilon^2$  permits a definition of roughness loss per unit distance per square roughness amplitude:

$$L_{Sm} = 10^{-6} L_{Rm} / \epsilon^2 = -8.68589 (10^{-6}) \operatorname{Im}[J(\mu_m, \kappa)] \text{ (dB/km/m}^2\text{)} \quad (4-33)$$

where  $\epsilon$  is in meters.

Equations 4-32 and 4-33 can also be used when the  $\mu_m(\epsilon)$  are found directly from a search using the determinant of the equivalent matrix. In that case,  $\Delta\mu_m = \mu_m(\epsilon) - \mu_m^{(0)}$  is used in Equation 4-32, leading to

$$L_{Sm} = -8.68589 (10^{-6}) \operatorname{Im}[\mu_m(\epsilon) - \mu_m^{(0)}] / \epsilon^2 \text{ (dB/km/m}^2\text{)} \quad (4-34)$$

$L_{Sm}$  is particularly significant for trapped modes in a surface duct. For propagation over smooth earth, these modes experience little or no attenuation in the propagation direction, which accounts for the field enhancement within the duct (Reference 1-4). For trapped modes within a surface duct characterized by a bilinear refractivity profile,

$$L_{Sm} \approx 1.0857 (10^{-6}) |\tan \alpha_1| k_0^2 (\lambda/d)^{1/2} (2 - \lambda/d)^{1/2} \text{ (dB/km/m}^2\text{)}, d > \lambda/2 \quad (4-35)$$

where  $\lambda$  and  $d$  are in the same units, and  $k_0 = m_0 k$  and  $\tan \alpha_1$  are in units of  $\text{km}^{-1}$ .  $L_{Sm}$ , as given in Equation 4-35, is always positive. This demonstrates that the roughness causes attenuation of the trapped modes. Equation 4-35 is valid for both the complete scattering (see Equation 4-27) and the partial scattering (see Equation 4-31) situations.

SECTION 5  
DISCUSSION AND RESULTS

To illustrate the effects of the roughness on the modes of propagation, plots are provided in Figure 5-1 of  $L_{Sm}$  as a function of the roughness spatial period  $d$  for the two trapped modes that are obtained when the surface duct refractivity profile of Figure 5-2 is used.  $L_{Sm}$  in these plots is calculated by two methods: the eigenvalue perturbation method using Equation 4-33 and the equivalent determinant method using Equation 4-34. A frequency of 6.814 GHz is used, corresponding to  $\lambda = 4.4$  cm. This figure shows that the eigenvalue perturbation results for the two trapped modes are identical, consistent with the usage of Equation 4-35, which is independent of the index  $m$  and which was originally derived from eigenvalue perturbation results. Indeed, the eigenvalue perturbation plot for the trapped modes is virtually identical with the closed form prediction of Equation 4-35.

It is emphasized that the trapped mode results shown in Figure 5-1 are unique to a surface duct. Values of  $L_{Sm}$  for trapped modes in an elevated duct were found to be several orders of magnitude lower, as would be expected since the ground roughness would not influence trapped mode propagation in an elevated duct.

A discrepancy is obvious in Figure 5-1 between the eigenvalue perturbation and the equivalent matrix results for the trapped modes as  $d/\lambda$  decreases. This corresponds to an increase in the size of the expansion parameter  $\Delta\bar{R}$ , as noted in the discussion following Equation 4-20. Although the two methods provide the same degree of accuracy, both are valid only for small values of the expansion parameter. Beyond this region of validity, there is no reason to expect the results of each method to be similar. The closeness of  $\Delta\bar{R}$  to zero, or the closeness of  $\bar{R}$  to  $-1$ , thus provides an indication of the accuracy of the expansion. Figure 5-3 illustrates the complex value of  $\bar{R}$  for the lowest order trapped mode, for  $\epsilon = 0.1$  m and various values of  $d/\lambda$ . The correlation between the distance of the  $\bar{R}$  values from  $-1$  and the divergence of the results of the two computational methods is obvious.

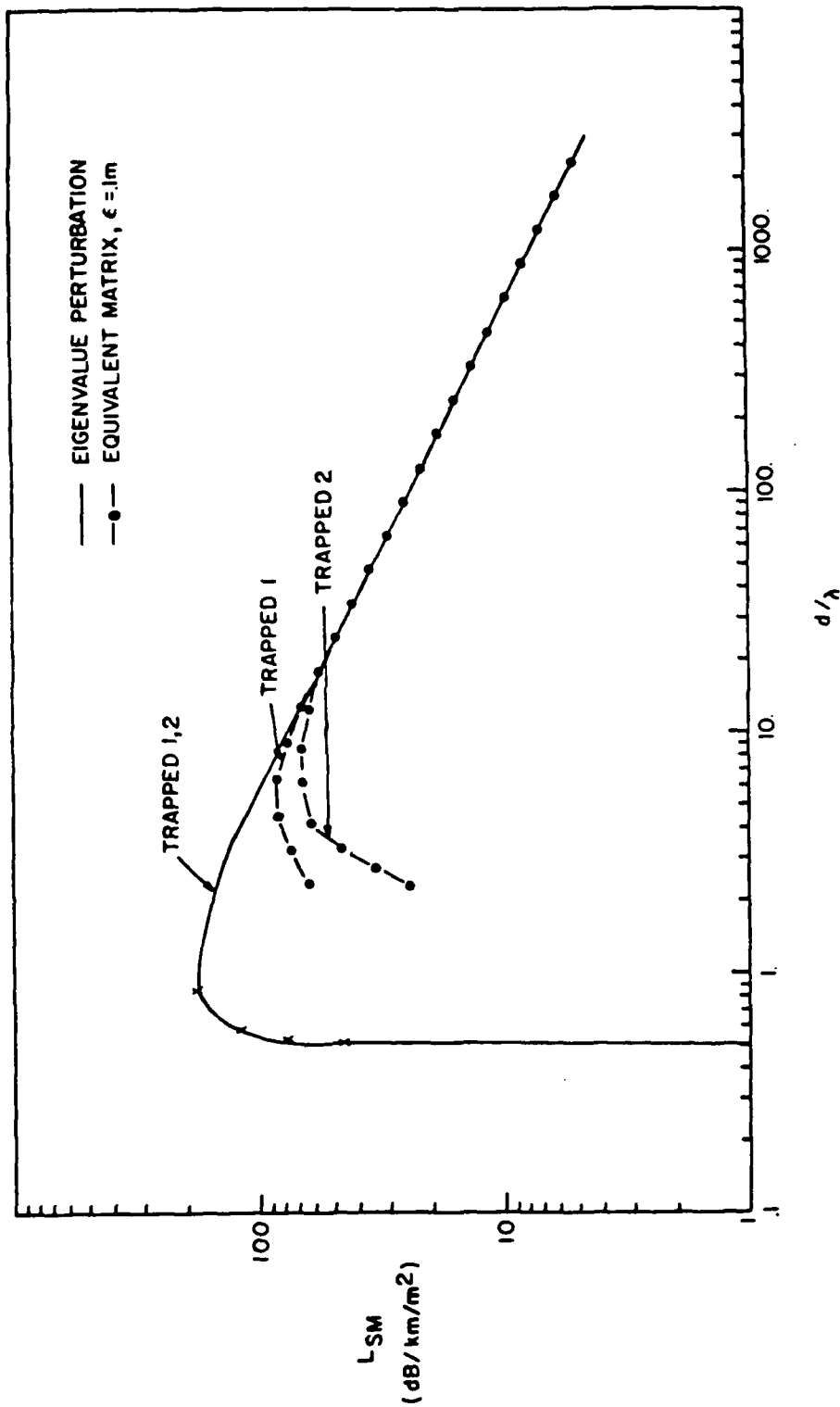


Figure 5-1. Roughness loss rate  $L_{SM}$  as a function of  $d/\lambda$  for trapped propagation modes within duct of Figure 5-2, using each of the computational models.

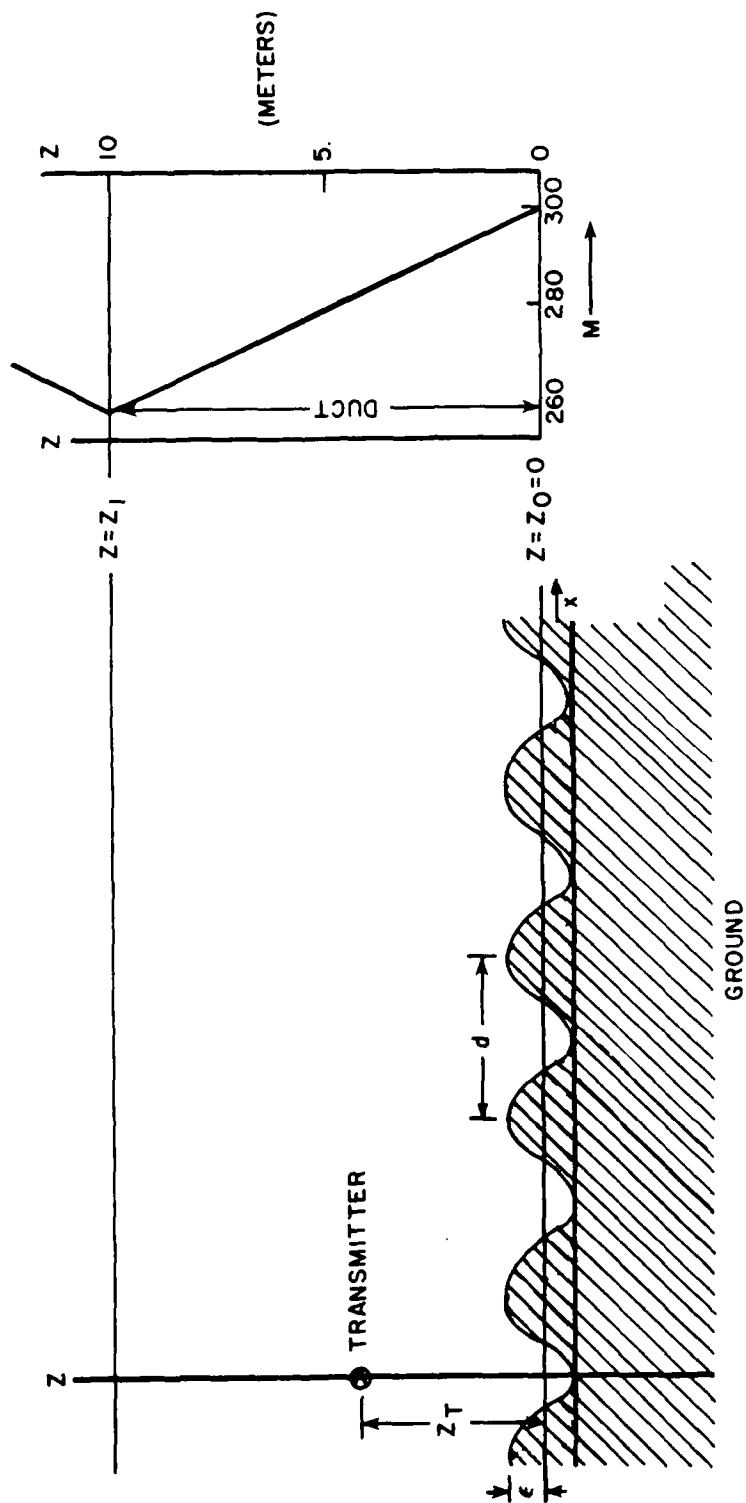


Figure 5-2. Physical model for duct calculations over sinusoidal rough earth.

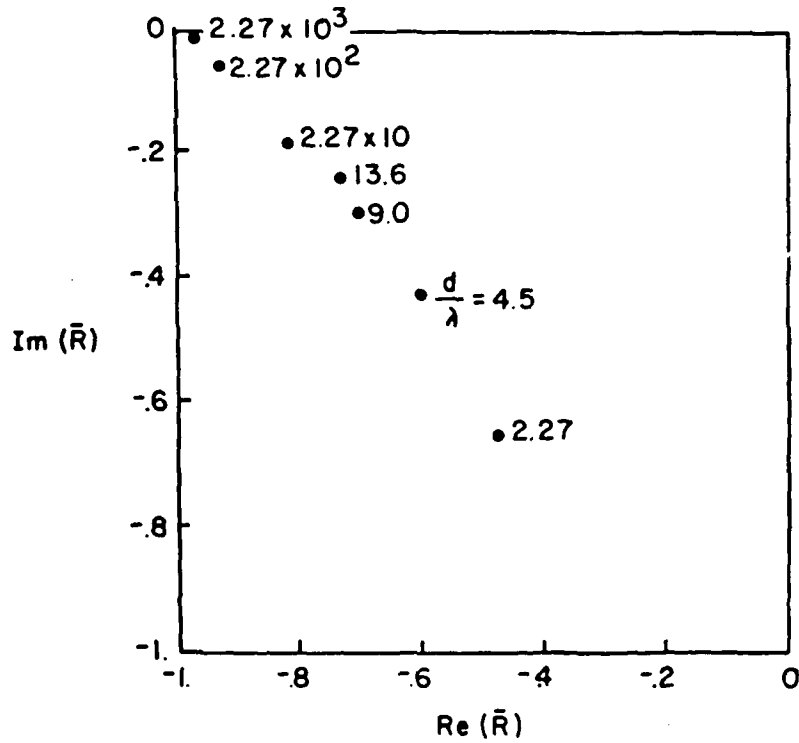
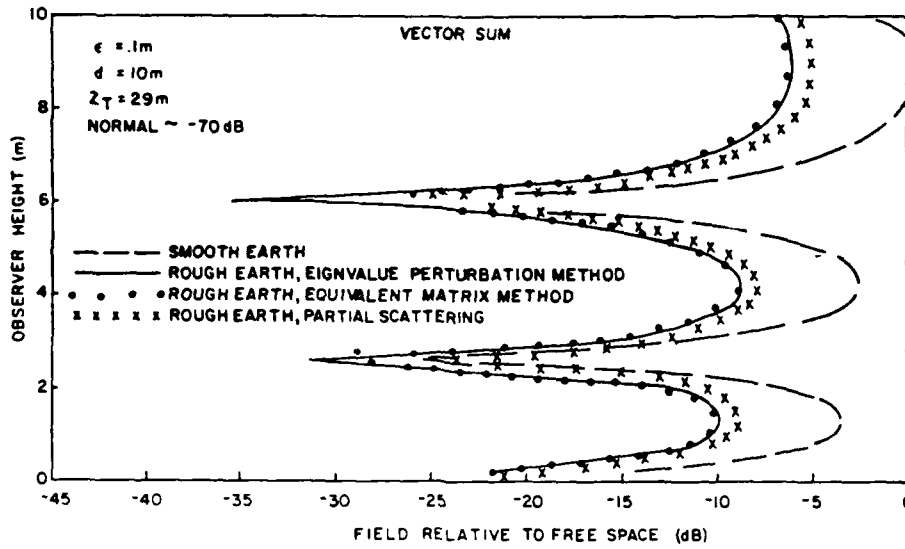


Figure 5-3. The effective reflection coefficient of sinusoidal ground for amplitude  $\epsilon = 0.1$  m, frequency = 6.814 GHz for different values of  $d/\lambda$ .

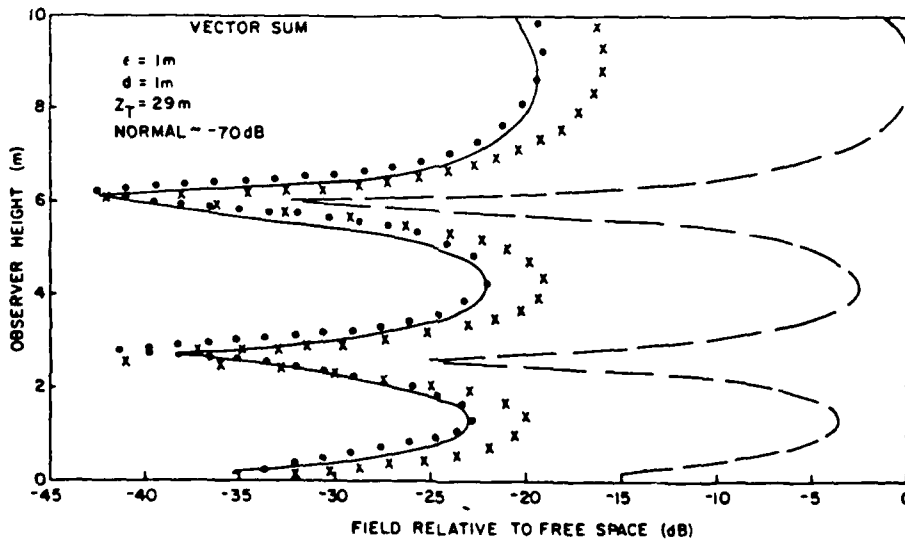
Predictions of the field relative to free space, using the four lowest order modes, are shown in Figure 5-4 for a 6.814 GHz radio wave propagating within the duct defined by the refractivity profile of Figure 5-2. They are illustrated as a function of observer height at a distance 66.7 km from the source for propagation over smooth earth and for three methods of computation for propagation over the sinusoidal rough earth: (1) the equivalent matrix method using the entire reflection coefficient correction, (2) the eigenvalue perturbation method using the entire reflection coefficient correction (i.e., Equation 4-27), and (3) the eigenvalue perturbation method using the partial reflection coefficient (i.e., using Equation 4-31). The rough earth is characterized by  $\epsilon = 0.1$  m.

For the predictions in Figure 5-4a, the source height  $z_T = 29$  m and  $d = 10$  m, while in Figure 5-4b,  $d = 1$  m with the same source height. In both figures, there is good agreement between the predictions obtained using methods (1) and (2). The discrepancy between these predictions and the partial reflection predictions is greater for the smaller value of  $d$ . Since the source is well above the duct, only the leaky mode contributes to the field. This mode is the third of the lowest order modes, thereby explaining the three peaks in the plots.

In Figure 5-4c,  $z_T = 5$  m and  $d = 10$  m. Since the entire contribution is now due to trapped modes that are the two lowest order modes, only two peaks are apparent in the plots. Here, there does not appear to be good agreement between any of the rough-earth results. Figure 5-4d is the comparison of the power sum results (Equation 4-7). Agreement in this figure, as well as the fact that the  $L_{Sm}$  in Figure 5-1 for each method is virtually identical, indicates that a major source of the problem is due to the relative phase of each mode. When the modal contributions are added without considering their phase, the agreement between the two complete reflection coefficient results improves except near the null.



(a)



(b)

Figure 5-4. Field relative to free space within duct of Figure 5-2  
 $f = 6.814 \text{ GHz}$ ,  $|x| = 66.7 \text{ km}$ , over smooth earth and over sinusoidal rough earth,  $\epsilon = 0.1 m$ . (Page 1 of 2).

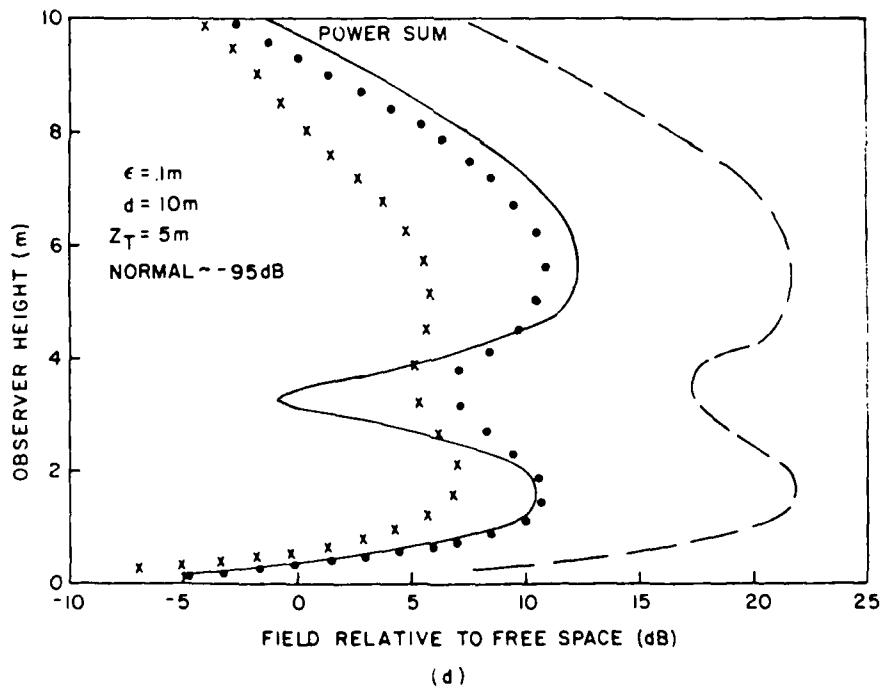
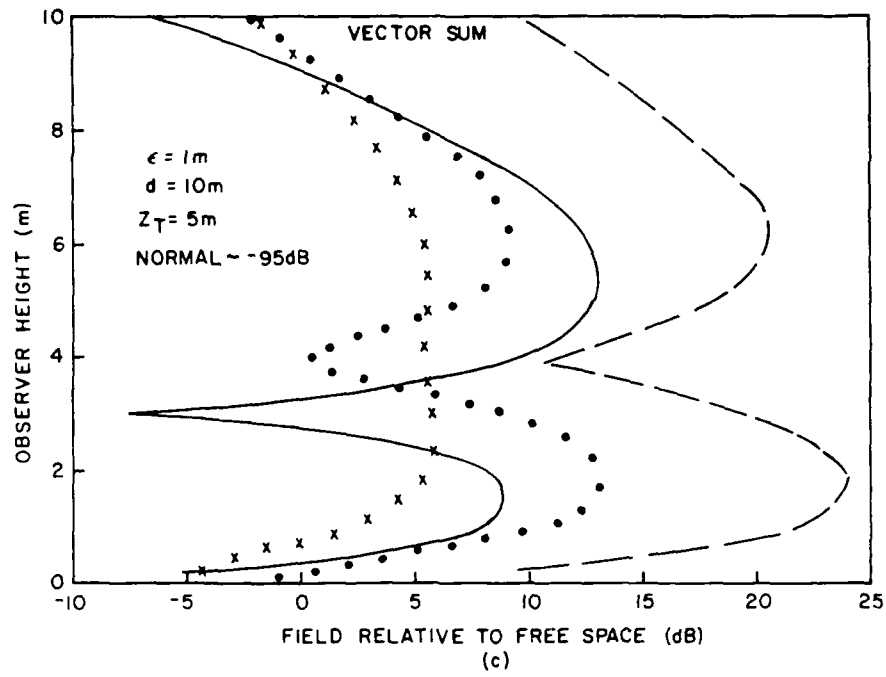


Figure 5-4. (Page 2 of 2).

SECTION 6  
SUMMARY

A method has been described for obtaining the effect of small sinusoidal roughness on horizontally polarized waves that are propagating in a surface duct situated over large distances in a horizontally homogeneous atmosphere. The method includes energy scattered out of, as well as into, the specular direction of modes of the corresponding smooth-earth waveguide.

It was shown that an eigenvalue perturbation scheme is as accurate as directly obtaining the eigenvalues from the equivalent matrix but requires much less computation time. The relationship between the two methods has been detailed, and the eigenvalue perturbations, as well as roughness loss rates, have been shown to be consistent with results obtained using a rough-earth form of the fundamental waveguide mode equation.

The methods documented in this report are a first step toward developing a mathematical model of propagation under the given conditions. They can be considered a research model applicable to a limited set of circumstances. Further work is needed to extend the model and make it more widely applicable.

## LIST OF REFERENCES

- 1-1. Kerr, D. E., "Propagation of Short Radio Waves," MIT Radiation Laboratory Series, Vol. 13, McGraw-Hill, New York, 1951.
- 1-2. Rotheram, S., "Radiowave Propagation in the Evaporation Duct," The Marconi Review," Vol. 37, No. 192, 1974, pp. 18-40.
- 1-3. Marcus, S. W., "A Model to Calculate EM Fields in Tropospheric Duct Environments at Frequencies through SHF," Radio Science, Vol. 17, No. 5, 1982, pp. 885-901.
- 1-4. Marcus, S. W., and Stuart, W. D., A Model to Calculate EM Fields in Tropospheric Duct Environments at Frequencies through SHF, ESD Technical Report 81-102, AD-A107710, DoD ECAC, Annapolis, MD, September 1981.
- 1-5. Budden, K. G., The Wave Guide Mode Theory of Wave Propagation, Logos Press, Ltd., London, 1961.
- 1-6. Hitney, H., et al., "Tropospheric Radio Propagation Assessment," Proceedings of the IEEE, Vol. 73, No. 2, 1985, pp. 265-283.
- 1-7. Rice, S. O., "Reflection of Electromagnetic Waves from Slightly Rough Surfaces," in The Theory of Electromagnetic Waves, M. Kline, ed., Interscience Publishers, New York, NY, 1951, p. 351.
- 1-8. Ament, W. D., "Toward a Theory of Reflection by a Rough Surface," Proceedings of the IRE, Vol. 41, No. 1, 1953, pp. 142-146.
- 1-9. Beard, C. I., "Coherent and Incoherent Scattering of Microwaves from the Ocean," IRE Transactions on Antennas and Propagation, Vol. AP-9, No. 5, 1961, pp. 470-483.
- 1-10. Marcus, S. W., "Propagation in a Surface Duct Over a Two-Dimensional Sinusoidal Earth," Radio Science, Vol. 23, No. 6, 1988, pp. 1039-1047.
- 2-1. Harvard Computational Laboratory, Tables of Modified Hankel Functions of Order One-Third and of Their Derivatives, Harvard University Press, Cambridge, MA, 1945.
- 3-1. Fessenden, D. E., "Space Wave Field Produced by a Horizontal Electric Dipole above a Perfectly Conducting Sinusoidal Ocean Surface," Third International Conference on Antennas and Propagation ICAP 83, 1983.

DISTRIBUTION LIST FOR  
 AN ANALYSIS OF PROPAGATION IN A SURFACE DUCT  
 OVER A PERIODICALLY ROUGH EARTH  
 ECAC-TR-88-001  
 (Page 1 of 3)

<u>External</u>	<u>No. of Copies</u>
Superintendent Naval Postgraduate School Monterey, CA 93940	1
Commander Naval Ocean Systems Center Attn: Dr. J. Rockway (Code 8105) San Diego, CA 92152	1
Commander Naval Ocean Systems Center Attn: H. V. Hitney San Diego, Ca 92152	1
M. R. Dresp MITRE Corp. P.O. Box 208 Bedford, MA 01730	1
John L. Skillman NSA/R521 Fort Meade, MD 20755	1
Douglas R. Woods NSA/R521 Fort Meade, MD 20755	1
Frank T. Wu Michaelson Laboratory Naval Weapons Center China Lake, CA 93555	1
Perry Snyder Code 5325 Naval Ocean Systems Center San Diego, CA 92152	1

DISTRIBUTION LIST FOR  
ECAC-TR-88-001  
(Page 2 of 3)

<u>External</u>	<u>No. of Copies</u>
Prof. James R. Wait Department of Electrical Engineering The University of Arizona Tucson, AZ 85721	1
Prof. L. B. Felsen Department of Electrical Engineering Polytechnic Institute of New York Route 113, Farmingdale, NY 11735	1
R. A. Pappert Naval Ocean Systems Center San Diego, CA 92152	1
Prof. Ezekial Bahar Electrical Engineering Department University of Nebraska Lincoln, NB 68588	1
Jeffrey Knorr Naval Post Graduate School Monterey, CA 93940	1
Dr. Russell Clarke DSTO Radiowave Propagation Electronics Research Laboratory P.O. Box 1600, Salisbury South Australia 5108	1
Harry Ng FSSM National Telecommunications and Information Administration 179 Admiral Cochrane Dr. Annapolis, MD 21401	1
W. Frazier FSSM National Telecommunications and Information Administration 179 Admiral Cochrane Dr. Annapolis, MD 21401	1

DISTRIBUTION LIST FOR  
 ECAC-TR-88-001  
 (Page 3 of 3)

<u>External</u>	<u>No. of Copies</u>
Defense Technical Information Center Cameron Station Alexandria, VA 22314	12
Dr. L. B. Wetzel, Sr. Scientist Code 5303 Naval Research Laboratories Washington, DC 20375-5000	2
 <u>Internal</u>	
XMTC/T. Treadway	5
DO/S. Cameron	1
DQI/R. Crawford	1
DQT/R. Whiteman	1
DC/K. Kontson	1
DCB/R. Meidenbauer	1
DCC/D. Lowe	1
DCF/G. Romanowski	1
DF/S. Kennison	1
DFA/S. Sorci	1
DFB/H. Knowlton	1
DFI/J. Borders	1
DFS/S. Timerman	1
DJA/J. Smithmyer	1
DN/D. Baran	1
DNA/N. Williams	1
DNM/P. Sautter	1
DNN/G. King	1
DR/A. Fitch	1
DRC/B. Lindsey	1
DRD/H. Riggins	1
DRD/M. Haberman	1
DRD/D. Eppink	1
DRD/S. Marcus	1
DRD/W. Stuart	1
DRI/M. McGarry	1
DRS/D. Williamson	1
DRS/P. Masters	1
DS/C. Gettier	1
DSA/P. Kubaryk	1
DSB/J. Copeland	1
DST/J. Benischek	1
DQL	10
DQL	Camera-Ready